REPORT FOR BOREHOLE EXPLOSION DATA ACQUIRED IN THE 1999 LOS ANGELES REGION SEISMIC EXPERIMENT (LARSE II), SOUTHERN CALIFORNIA: PART I, DESCRIPTION OF THE SURVEY

by Gary S. Fuis[1], Janice M. Murphy[1], David A. Okaya[2], Robert W. Clayton[3], Paul M. Davis[4], Kristina Thygesen[5], Shirley A. Baher[4], Trond Ryberg[6], Mark L. Benthien[2], Gerry Simila[7], J. Taylor Perron[1], Alan K. Yong[1], Luke Reusser[2], William J. Lutter[8], Galen Kaip[9], Michael D. Fort[10], Isa Asudeh[11], Russell Sell[1], John R. Vanschaack[12], Edward E. Criley[12], Ronald Kaderabek[12], Will M. Kohler[1], Nickolas H. Magnuski[1]

Open-File Report 01–408

2001

This report is preliminary and has not been reviewed for conformity with U.S. Geological Survey editorial standards or with the North American Stratigraphic Code. Any use of trade, firm, or product names is for descriptive purposes only and does not imply endorsement by the U.S. Government.

U.S. DEPARTMENT OF THE INTERIOR
U.S. GEOLOGICAL SURVEY

[1] U.S. Geological Survey, Menlo Park, CA 94025
[2] Southern California Earthquake Center, University of Southern California, Los Angeles CA, 90089-0740
[3] Southern California Earthquake Center, University of California at Los Angeles, Los Angeles, CA 90024-1567
[4] Southern California Earthquake Center, California Institute of Technology, Pasadena, CA 91125
[5] Copenhagen University, Copenhagen, DENMARK1350; TK 170573
[6] GeoForschungsZentrum, Potsdam, 14473 GERMANY
[7] Southern California Earthquake Center, California State University at Northridge, Northridge, CA 91330
[8] University of Wisconsin-Madison, Madison, WI 53711
[9] University of Texas at El Paso, El Paso, TX 79968-0555
[10] IRIS/PASSCAL, Socorro, NM 87807
[11] Geological Survey of Canada, Ottawa, CANADA K1A 0Y3
[12] U.S. Geological Survey, Menlo Park, CA 94025 (retired)

TABLE OF CONTENTS

APPENDICES

TABLES

FIGURES

FIGURES (continued)

INTRODUCTION

The Los Angeles Region Seismic Experiment (LARSE) is a joint project of the U.S. Geological Survey (USGS) and the Southern California Earthquake Center (SCEC). The purpose of this project is to produce seismic images of the subsurface of the Los Angeles region down to the depths at which earthquakes occur, and deeper, in order to remedy a deficit in our knowledge of the deep structure of this region. This deficit in knowledge has persisted despite over a century of oil exploration and nearly 70 years of recording earthquakes in southern California. Understanding the deep crustal structure and tectonics of southern California is important to earthquake hazard assessment. Specific imaging targets of LARSE include (a) faults, especially blind thrust faults, which cannot be reliably detected any other way, and (b) the depths and configurations of sedimentary basins. Imaging of faults is important in both earthquake hazard assessment but also in modeling earthquake occurrence. Earthquake occurrence cannot be understood unless the earthquake-producing "machinery" (tectonics) is known (Fuis and others, 2001). Imaging the depths and configurations of sedimentary basins is important because earthquake shaking at the surface is enhanced by basin depth and by the presence of sharp basin edges (Wald and Graves, 1998, Working Group on California Earthquake Probabilities, 1995; Field and others, 2001). (Sedimentary basins are large former valleys now filled with sediment eroded from nearby mountains.) Sedimentary basins in the Los Angeles region that have been investigated by LARSE include the Los Angeles, San Gabriel Valley, San Fernando Valley, and Santa Clarita Valley basins.

The seismic imaging surveys of LARSE include recording of earthquakes (both local and distant earthquakes) along several corridors (or transects) through the Los Angeles region and also recording of man-made sources along these same corridors. Man-made sources have included airguns offshore and borehole explosions and vibrating-truck sources onshore. The two chief LARSE transects pass near recent moderate earthquakes, including the 1971 M 6.7 San Fernando, 1987 M 5.9 Whittier Narrows, 1991 M 5.8 Sierra Madre, and 1994 M 6.7 Northridge earthquakes. The first transect extended from San Clemente Island northeastward to the Mojave Desert (Line 1, Fig.1), passing near the epicenter of the Whittier Narrows and Sierra Madre earthquakes. The second transect extended from west of San Clemente Island northward to the western Mojave Desert (Line 2, Figs. 1, 2), passing through the epicenter of the Northridge earthquake and near the epicenter of the San Fernando earthquake. Data along Line 1 were acquired during the years 1993-1994, and data along Line 2, during the years 1994-2000.

In this open-file report and that of Murphy and others (in preparation), we present the details of the October 1999 explosion survey along Line 2, which extended from Santa Monica Bay northward to the western Mojave Desert (Figs. 1, 2). This survey is referred to as LARSE II. In this survey, 93 borehole explosions were detonated along the main north-south line and along 5 auxiliary lines in the San Fernando Valley and Santa Monica areas. These explosions were recorded by ~1400 seismographs. Prior LARSE surveys include the following:

(1) 1993 recording of local and distant earthquakes along Line 1 (1-month period) (Kohler and others, 1996)

(2) 1994 recording of airgun signals on a 4.2-km-long seismic streamer towed by the R.V. Ewing along the offshore parts of Lines 1, 2, and 3 (Brocher and others, 1995)
(3) 1994 recording of airgun signals on ocean-bottom seismographs along the offshore parts of Lines 1 and 2 (ten Brink and others, 1996)
(4) 1994 onshore recording of the airgun signals along Lines 1, 2, and 3 (Okaya and others, 1996a)
(5) 1994 onshore recording of earthquakes along Lines 1, 2, and 3 (8-day period) (Okaya and others, 1996b).
(6) 1994 recording of borehole explosions along Line 1 (Murphy and others, 1996)
(7) 1997 recording of local and distant earthquakes along Line 1 in the Los Angeles basin (9-month period) (Kohler and others, 2000)
(8) 1998-1999 recording of local and distant earthquakes along Line 2 (6.5-month period) (Kohler and Kerr, in preparation)

A variety of seismic instrumentation was used in these imaging surveys and was obtained from collaborators from around the world, including the Geological Survey of Canada (Ottawa, Canada), IRIS/PASSCAL (Socorro, NM), Lamont-Doherty Earth Observatory (Palisades, NY), Stanford University (Stanford, CA), SCEC (Los Angeles, CA), USGS (Menlo Park, CA, and Woods Hole, MA), University of Texas at El Paso (El Paso, TX), GeoForschungsZentrum (Potsdam, Germany), University of Karlsruhe (Karlsruhe, Germany), and University of Copenhagen (Copenhagen, Denmark). The reader is referred to Table 1 for instrumentation used in LARSE II.

GEOLOGIC SETTING

The LARSE II survey extended northward from Santa Monica Bay through the Santa Monica Mountains, San Fernando Valley, Santa Susana Mountains, Santa Clarita Valley, north-central Transverse Ranges, and western Mojave Desert, with a sparsely recorded extension into the Sierra Nevada (Figs. 2-5). The survey also included 3 auxiliary lines in the San Fernando Valley basin and 2 auxiliary lines in the Santa Monica area. Chief faults we hoped to image in the LARSE II survey include, from south to north, the Santa Monica fault, the causative fault for the Northridge earthquake, the Northridge Hills fault, the Santa Susana thrust fault, the San Gabriel fault, and the San Andreas fault. Sedimentary basins we hoped to image include the San Fernando Valley and Santa Clarita Valley basins. Below, we describe the geologic setting for each geologic region crossed by LARSE II lines.

The Los Angeles basin is a rift basin that began to form perhaps as early as the Paleogene but took on its modern configuration in late Miocene through Pleistocene times (Wright, 1991; McCulloh and others, 2000). It is located at the juncture of three primary physiographic provinces of southern California, the Transverse Ranges, the Peninsular Ranges, and the Continental Borderland (Fig. 1), and shares the geologic history of all three provinces. Structurally, it is bounded by the current left-oblique Santa Monica/Hollywood fault system on the north, the right-oblique Whittier fault on the northeast, and the right(?)-oblique Palos Verde fault on the southwest. These modern faults are believed to have superseded normal faults that existed during a period of rifting/ transtension prior to 3.9-3.4 ma (Wright, 1991; Crouch and Suppe, 1993). The rifting apparently involved clockwise rotation of the western Transverse Ranges, including the Santa

Monica Mountains, of more than 90 degrees from positions on the current Continental Borderland to their present positions (Hornafius and others, 1986, Crouch and Suppe, 1993). In its center, south of Los Angeles, the Los Angeles basin contains as much as 10 km of Miocene and younger sedimentary rocks (Yerkes and others, 1965; Fuis and others, 2001). In the Santa Monica area, where two LARSE II auxiliary lines are located, the Los Angeles basin contains 3 km or more of sedimentary rocks that are juxtaposed across the Santa Monica fault with the Santa Monica Slate, Mesozoic granitic rocks, and a low-angle-faulted stack of Upper Cretaceous through Miocene sedimentary and volcanic rocks.

The Santa Monica Mountains are Mesozoic metamorphic rocks (Santa Monica Slate) and granitic rocks overlain by a section of Upper Cretaceous to Miocene clastic sedimentary and volcanic rocks, with some diabasic intrusive rocks (Campbell and others, 1966; Jennings and Strand, 1969; Yerkes and Campbell, 1980; Dibblee, 1992). The structure is a west-plunging antiform where Line 2 crosses it, but structure within the Mesozoic-Cenozoic sedimentary rocks is debated. Campbell and others (1966) interpret a stack of several thrust sheets within the sedimentary section, but the sense of stacking is always younger over older, and could represent, instead, simple unconformities or detachment faulting. Detachment faulting is predicted in the model of Crouch and Suppe (1993), wherein the Los Angeles basin and inner Continental Borderland (Fig. 1) were extended in the Neogene as the western Transverse Ranges, including the Santa Monica Mountains, rotated (by more than 90 degrees) from positions in the current Continental Borderland to their present positions. Core complexes were created in the center of the rift (e.g., Santa Catalina Island (Fig. 1) and the Palos Verde peninsula) and detachment faults are observed chiefly on the edges of the Santa Monica Mountains, western Peninsular Ranges and southeastern part of the inner Continental borderland (Crouch and Suppe, 1993).

The San Fernando Valley, located within the western Transverse Ranges, is structurally the southeastward echelon extension of the east-trending Ventura basin. In the southern part of the valley, a Miocene to Holocene clastic sedimentary section overlies a basement containing granitic rocks penetrated by oil wells at depths of 1.3-1.4 km (Tsutsumi and Yeats, 1999). These granitic rocks are similar to those exposed in the Santa Monica Mountains to the south. In the northern and northeastern part of the valley, basement is not penetrated by oil wells (some wells as deep as 3 km), except near the west end of the crystalline San Gabriel Mountains. Gravity modeling, geologic projection from outcrops, and oil-well data indicate a depth to basement exceeding 3-4 km (Oakeshott, 1975; Weber, 1975; Langenheim and others, 2000; Tsutsumi and Yeats, 1999). The thickness' of individual sedimentary formations increase significantly in the northern part of the valley and to the north in the Santa Susana Mountains. Abrupt thickness changes are seen across the western and central Santa Susana thrust fault, mid-slope on the south side of the Santa Susana Mountains (Winterer and Durham, 1954; Yeats, 1987), and the Mission Hills reverse fault, at the base of the Santa Susana Mountains (Tsutsumi and Yeats, 1999) (see Fig. 2). These two faults were apparently formed during the Pliocene along normal faults or hingelines for the deep eastern part of the Ventura basin to the north.

Historic faulting in and beneath the San Fernando Valley has occurred along conjugate reverse faults, the north-dipping San Fernando fault, which ruptured from a depth of 13-15 km beneath the eastern Santa Clarita Valley (Soledad Canyon) to the surface in the northeastern San Fernando Valley in the 1971 M 6.7 San Fernando earthquake (Allen and others, 1971, 1975; U.S.

Geological Survey staff, 1971: Heaton, 1982), and the south-dipping Northridge fault, which ruptured from a depth of 18-19 km in the southern San Fernando Valley to a depth of 5-8 km in the northern part of the valley (Hauksson and others, 1995; Mori and others, 1995). The northeastern part of the Northridge aftershock zone is apparently truncated by the southwestern part of the San Fernando aftershock zone (Mori and others, 1995; Tsutsumi and Yeats, 1999). Tsutsumi and Yeats (1999) suggest that the San Fernando fault zone actually extends at depth southwestward of the 1971 surface breaks to the Northridge Hills fault, and they interpret the 1971 surface breaks and the Mission Hills fault as upward splays from this southward extension.

The sedimentary rocks of the eastern Ventura basin have been uplifted in the central and northern Santa Susana Mountains and in the low hills and valleys south of the San Gabriel fault in the Santa Clarita Valley (see Figs. 2, 3). The Upper Miocene through Quaternary sedimentary section is substantially thicker here than in the San Fernando Valley south of the Santa Susana and Mission Hills faults, as stated above. Gravity modeling and geologic projection from oil-well data indicate that basement depth ranges from 1.5 to possibly 4 km (Winterer and Durham, 1954; Stitt, 1986; Yeats and others, 1994; Dibblee, 1996).

The San Gabriel fault is an older branch of the San Andreas fault system, that was active during the period ~10-5 Ma and has a total offset of 40-60 km in the region of Line 2 (Crowell, 1962, 1982; Bohannon, 1975; Ehlig and others, 1975; Powell, 1993). It separates the Soledad and Ridge sedimentary basins on the north and east from the eastern Ventura basin and older rocks on the south and west. There is a marked difference between the basin histories north and south of this fault, and these basins were clearly formed in separate environments (Crowell, 1954, 1962, 1982; Jahns and Muehlberger, 1954; Winterer and Durham, 1954). The Soledad basin contains Oligocene through Quaternary sedimentary rocks and wraps around the south side of the Sierra Pelona to interfinger with the base of the Upper Miocene and Pliocene Ridge basin. Along Line 2, Stitt (1986) and Dibblee (1996) show a ridge of basement rocks (granitic and metamorphic rocks, based on oil-well data) at 1- to 3-km depth in the northeasternmost part of the Ventura basin, just south of the San Gabriel fault. Basement depth (> 3 km) to the north, beneath the western Soledad basin is unknown. Basement rocks (Pelona Schist) are exposed at the surface along Line 2 farther north, across the Sierra Pelona fault (see Figs. 3, 4).

Sierra Pelona, Sawmill Mountain, and Liebre Mountain are echelon basement terranes bounded on the northeast by the San Andreas fault system and on the south and southwest by older faults of various ages that extend into the Soledad and Ridge basins. These faults include (1) the Sierra Pelona fault, located along the south side of the Sierra Pelona, (2) the San Francisquito fault, along the north side of the Sierra Pelona, buried by upper Miocene strata of the Ridge basin, (3) the Clearwater fault along the south edge of the Sawmill Mountain block, that is buried by the middle part of the Ridge basin section, and (4) the Liebre fault, along the south side of the Liebre Mountain block, that is buried by the uppermost part of the Ridge basin section (Crowell, 1954; Jahns and Muehlberger, 1954; Jennings and Strand, 1969). The San Francisquito fault is part of the earliest San Andreas fault system in southern California (see summary in Powell, 1993). The San Francisquito fault and Pelona Schist of the Sierra Pelona are offset ~45 km right laterally within the San Andreas fault system from a similar structure and from similar rocks in the northern San Gabriel Mountains (Ehlig, 1968, 1981; Powell, 1993). The Liebre fault, which bounds a distinctive intrusive rock type in the Liebre Mountains, is in part a thrust fault believed to be equivalent to, and offset from, the Squaw Peak thrust fault in the western San Bernardino Mountains. The Squaw Peak thrust fault lies 160 km to the southeast, on the north side of the San Andreas fault system (Matti and others, 1985; Meisling and Weldon, 1989). A wedge of Paleocene to Oligocene-aged sedimentary rocks of unknown origin and structural thickness lies between the San Francisquito and Clearwater faults.

North of the San Andreas rift zone along Line 2, is a low ridge of Mesozoic granitic rocks which is overlain to the north in the western Mojave Desert by Oligocene and younger sedimentary and volcanic rocks (Dibblee, 1967). An oil test well in the western Mojave Desert, located near Line 2 ~85 km north of the coast, reaches basement (granitic rocks) at 2.4-km depth. Beginning about 104 km north of the coast, Line 2 is underlain by igneous and metamorphic rocks of the northwestern Mojave Desert and Tehachapi Mountains (Dibblee, 1967). Line 2 crosses the Garlock fault at about 109 km north of the coast and terminates in granitic rocks in the southern Sierra Nevada 150 km north of the coast.

EXPERIMENT PLANNING AND DESIGN

The geographic location of Line 2 was actually chosen prior to the January 1994 M 6.7 Northridge earthquake and was based on our desires to (a) cross the western Transverse Ranges more or less perpendicularly to geologic strike, (b) provide an offshore extension of the route that passed near Santa Catalina and San Clemente Islands, (c) cross the San Fernando Valley through the aftershock zone of the 1971 San Fernando earthquake, (d) route the line through as many large open spaces as possible, for shotpoint location and background seismic noise reduction, and (e) locate the line along access roads, wherever possible. This route (Line 2) fortuitously passed through the epicentral area of the Northridge earthquake (Figs. 1-3).

Seismographs were deployed along the onshore part of Line 2 in 1994 to record airgun sources located along its offshore extension (Figs 1, 2) (Brocher and others, 1995; Okaya and others, 1996a). Local and distant earthquakes were recorded by seismographs deployed along Line 2 during a ~6-month period from November 1997 to April 1998 (Fig. 2) (Kohler and others, 2000). In the Fall of 1999, 93 borehole explosions were recorded by ~1400 seismographs along Line 2 and five auxiliary lines (Figs. 2-5; Tables 1, 2a).

The 1999 survey consisted of a 150-kilometer-long main line (Line 2) and five auxiliary lines, ranging in length from 11-22 km: three in the San Fernando Valley and two in the Santa Monica region (Figs. 1-5). The route of Line 2 through the San Fernando Valley was determined by the factors listed above, and especially by the location of the campus of California State University at Northridge, which provided one of the largest blocks of open space in the valley. Line 2 was designed to be a combined refraction/ low-fold reflection survey. A shotpoint spacing of 1 km and an instrument spacing of 100 m was our goal, and we nearly achieved this goal from the coast to the southern Mojave Desert (0-79 km). In that interval our average shotpoint spacing is 1.2 km and average station spacing is 103 m. North of that interval, shotpoint spacing averages 2.75 km from 79-101 km, and the remaining shotpoint on Line 2 (the northernmost shotpoint, SP 9136) was located at 136 km (see Figs. 1-5; Table 2a). Station spacing averages 100 m from 79 to 90 km, 300 m from 90 to 98 km, 500 m from 98 to 101 km, and 1000 m from 101 to 150 km (Figs.

4,5). Our goal for shot size was to mix small (113 kg, or 250 lbs.), medium (227 kg, or 500 lbs.), and large (454 kg, or 1000 lbs., and larger) shots, in order to investigate reflective features at all crustal and upper mantle depths and also to investigate reflective features with differing frequency returns (Fig. 6). In general, larger shots generate energy with lower frequency. Such a mixture was possible in areas of open space, including the several mountain ranges crossed, and also the Mojave Desert. In areas of dense population and in many other areas where buildings, aqueducts, and pipelines were nearby, shot size was determined as described below (see "Shotpoints and Shot Size Determination"). All shots on all lines were recorded by the seismographs on all lines, except for shots in the last two nights of shooting, where some instruments had memory limitations (Table 1).

The three short cross-lines in the San Fernando Valley were designed as refraction surveys and are informally named the "3000", "4000", and "5000" lines, after station numbers (Fig. 3). The 3000 and 4000 lines were designed to image the velocity structure along strike in the upper few km of the southern and northern parts of the San Fernando Valley, respectively. The 3000 line was located to take advantage of open space and access provided by the Sepulveda Flood Control basin, along the Los Angeles River. The 4000 line was designed to coincide in large part with an oil-industry seismic line along Devonshire Blvd (made available to SCEC, see Tsusumi and Yeats, 1999) and it's eastern end was located in the open space of the Hansen Dam Flood Control Basin. The 5000 line was designed to cross the Bouguer gravity low centered on the Van Norman Debris Basin in the northern San Fernando Valley (see Oliver and others, 1980). This line joined the eastern end of the 4000 line at Hansen Dam and intersected Line 2 at SP 8310. Along the 3000 line, 3 relatively large shots (136-295 kg, or 300-650 lbs.) were detonated in the central part of the line, and a smaller shot (SP 8170) was detonated near its west end on the main line. Four relatively large shots (227-455 kg, or 500-1000 lbs.) were detonated at a pair of shotpoints at both ends of the 4000 line (SP's 9211, 9212, 9221, 9222). Double shots were detonated with the intention of stacking the signals. Two smaller shots were detonated along the line--SP 9213 at or near the Verdugo fault and SP 8260 on the main line (Fig. 3). The 5000 line had only shots on its ends - the double shot at the eastern end of the 4000 line (SPs 9211, 9212) and a shot on the main line (SP 8310).

The 2 auxiliary lines in the Santa Monica area were designed to investigate the exaggerated shaking that occurred there during the 1994 M 6.7 Northridge earthquake (Gao and others, 1996; Davis and others, 2000). The 6000 line and a scatter deployment of 50 3-component Reftek recorders (Fig. 3) were deployed through the region of maximum damage. The 7000 line, which was designed as a control line, was deployed through an area with little or no damage to the east of and parallel to the 6000 line. Two large shots (SP's 9350 and 9360; 1700 and 1800 kg, respectively), located at azimuths similar to the azimuths of Northridge aftershocks showing the highest amplitudes in the damage zone and at distances that produced critical reflections from the Moho (approximately 70 and 90 km from the Santa Monica area, respectively), were detonated well west of Line 2 (Fig. 1, 2). These shots were designed to approximate upcoming rays from the Northridge shocks at Santa Monica (see Gao, and others, 1996). In addition, in-line shots were detonated on both the 6000 and 7000 lines. The 6000 line recorded 4 in-line shots, including a northern end shot on the main line (SP 8130), and the 7000 line recorded 2 in-line shots (Fig. 3). The scatter deployment in the damage zone was deployed as a passive survey a few days before the explosion survey, and some of these instruments fortuitously recorded the October 16, M 7.1 Hector Mine earthquake.

Seismographs used in LARSE II included 5 types with varied recording parameters (Table 1). The Reftek, Texan, SGR, and PDAS seismograph systems have broad bandwidths, from 4.5 Hz (sensor eigen frequency; 8 Hz for the SGR's) to more than 100 Hz. The PRS1's and PRS4's have narrow bandwidths, from 2 Hz (sensor eigen frequency) to about 20 Hz. The Refteks, and PRS4's are 3-component recorders. Three-component recorders were distributed as evenly as possible among all lines, including the main and auxiliary lines. Along Line 2, from 0-100 km, where we hoped to record near-vertical-incidence reflections, we chiefly used the broader-band instruments, and all instrument types were mixed, to the extent possible. From 0-100 km, Refteks were deployed at 500-600-m intervals on average. PDAS's were deployed continuously as 6-channel cabled spreads from 62-90 km, with one or more Refteks between each spread. Texans were interspersed throughout the line from 0-100 km, but, because of their small size, were deployed exclusively in hike-in segments of the line, notably from 29-30 km, 57-62.5 km, and 66.5-68.5 km. SGR's were interspersed from 0-57 km, averaging 600-700 m apart and PRS1's were interspersed every 1 km from 0-44 km. From 100-150 km, an interval with only 2 shotpoints, PRS1's were deployed at 1 km intervals with no other interspersed instruments. On the 3000 line, 11.4 km long, station spacing averaged 200 m. PRS4's (3-component) were deployed approximately every 400 m, or approximately at every other instrument site, with PRS1's, SGR's, and Texans at the remaining sites. On the 4000 line, 21.8 km long, station spacing averaged 270 m. PRS4's and Refteks were deployed approximately every 1200 m, or approximately every fourth or fifth instrument site, and the remainder of the sites were Texans, SGR's, and PRS1's. On the 5000 line, 12.4 km long, station spacing averaged nearly 400 m and only four 3-component instruments (Refteks) were deployed. On the 6000 line, 19.5 km long, station spacing averaged approximately 200 m, and Refteks were spaced on average every 880 m, or at every fourth or fifth instrument site. The scatter deployment of 50 instruments (all 3-component Refteks) was approximately 2.7-km in diameter and centered on downtown Santa Monica. On the 7000 line, 16.2 km long, station spacing averaged 300 m, and there were only five 3-component instruments (Refteks) on the line.

PERMITTING

Permitting was a lengthy process, lasting nearly 2 years. In all, 50 permits were required for 93 shotpoints, and 376 permits were required for over 1400 instrument locations (Table 3). Permits were received from 3 federal, 1 state, and 12 local government agencies, and from 3 conservation/education organizations, 20 commercial/industrial organizations, and 337 private citizens. All government agencies and all conservation/educational organizations that were approached ultimately granted the requested permits, and most commercial/industrial organizations and private citizens did likewise. Our worst results were from land developers, but 2 out of 6 ultimately granted the requested permits. We are very indebted to all agencies, organizations, and people who participated in LARSE II by granting permission and, in many cases, vital assistance to our survey. Commercial/industrial organizations and private citizens granted a total of 31 shotpoint permits (33 %) and 357 recorder permits (95%). Clearly, without the cooperation of these organizations and citizens, LARSE would have been less than a success.

As discussed in the above section, shotpoint locations were sought in open spaces, where shaking of nearby personal residences, buildings, and other structures would be minimized, and where, if possible, prior grading or other impacts on the land surface existed, such as in parking lots, road pullouts, and abandoned or seldom-used roads and trails. To the extent possible, instrument locations were also sought in open spaces, and along seldom-used roads and trails, where background seismic noise would be minimized; some spot measurements of seismic noise level were performed before site selection. In addition, security of instruments was of great importance, and sites were selected where instruments could be hidden or buried. In populated areas, such secure sites included the back yards and garden areas of many private citizens. All siting requests, for shotpoints and recorders, were accompanied with pamphlets and/or USGS Fact Sheets on LARSE (in English and Spanish) that were written specially for the permitting process (Henyey and others, 1999a, b). In addition, all shotpoint permit requests were accompanied by an environmental assessment (see Murphy and others, in preparation). Several government agencies and companies required more detailed estimates of ground shaking from our seismic shots (see "Shotpoints and Shot-Size Determination") below.

For shotpoints located on property managed by the City of Los Angeles, the shooting procedures were overseen by the City Engineer, City and County Fire Marshals, County Sheriff (Bomb Squad), and the California Occupational Safety and Health Administration (CALOSHA).

SHOTPOINTS AND SHOT-SIZE DETERMINATION

LARSE II shots were explosions detonated at the bottoms of drill holes measuring 20 cm (8 in) in diameter and more than 18 m (60 ft) deep (Table 2b; Fig. 7). The holes were drilled by a commercial water-well-drilling rig and cased as needed with iron pipe or, in some cases, with PVC. The explosive is a commercial ammonium-nitrate-based product (blasting agent) that is pumped into the drill hole by a pump truck. The total depth of each drill hole varies with charge size, according to the approximate formula:

hole depth (m) = 18 m + shot-size (kg)/37.3 kg/m
(or hole depth (ft) = 60 ft + shot-size (kg)/25 lbs/ft)

Holes are loaded as much as one month prior to detonation, but are not "primed" for detonation until minutes before actual detonation. Loading is accomplished as follows:

a) Hole depth and depth to water is measured.
b) A length of detonating cord that is slightly longer than hole depth is spooled out, and a weight is attached to one end.
c) Boosters (Class B explosive) are threaded onto the detonating cord and taped in place at the top and bottom of the interval to be occupied by the blasting agent. When

needed, boosters were taped at 3-m (10-ft) intervals along the cord between the top and bottom boosters.

c) The detonating-cord/booster assembly is lowered down the hole.

d) The required amount of blasting agent is pumped from a truck using a hose lowered to the bottom of the hole and slowly drawn upward during the pumping process.

e) A bag of dirt is lowered to the top of the blasting agent, at 18-m depth, to separate the blasting agent from fill or "tamp" above.

f) Drill cuttings or gravel are shoveled on top of the dirt bag, filling the hole nearly to the surface. Clean gravel is used in cases where the hole contains significant water. (Drill cuttings simply mix with the water and do not sink to efficiently contain the explosion.)

g) The detonating cord is wrapped around a locking bar, that is inserted through both the casing and a custom-made cap (Fig. 7).

h) Where the cap and casing protruded above ground, they were covered with a pile of dirt to avoid attracting attention.

In LARSE II, efficient loading, as described above, led to consistently energetic explosions, and to consistently good seismic data (see below). The explosions were detonated at night, when wind and cultural noise are at their lowest levels at seismograph sites. After inspecting the area for stray currents that might prematurely detonate an electrical blasting cap, each shot crew attached a cap to the detonating cord ~5 minutes before shot time. The cap was fired by a signal from a master clock and a shooting system designed by the USGS. The cap initiated successive detonation of the cord, boosters, and blasting agent. The shot times (Table 2a) are generally master-clock trigger times; delays for the caps, detonation cord, boosters, and blasting agent, which explode at ~5.5-6.0 km/s, are ignored. Master clocks generally drift less than 1 millisecond per week. For two LARSE II shots (SP's 8084 and 8270), stray currents were dangerously high and an alternate, percussive firing system was used. Shot times were estimated in these two cases using up-hole seismographs.

Where shotpoints were located near private residences, buildings, or other structures, shot size was determined using ground-shaking data collected in LARSE I plus data from a series of calibration shots (11, 23, and 68 kg in size) at SP 204C, in the San Fernando Valley (Fig. 8). [Note: since these amplitude data were needed in planning the LARSE II shot sizes, NO LARSE II DATA WERE USED IN MODELING SEISMIC AMPLITUDES.] A model curve was fitted through the seismic amplitudes (or, upward ground velocities) using the formula of Kohler and Fuis (1992):

$$a_{ij} = b_1 x_{ij} + b_2 x_{ij}^2 + c_1 w_i + g_X$$

where:

a_{ij} is the logarithm (base 10) of the seismic amplitude for the ith shot and jth trace, (in units of cm/s),

x_{ij} is the logarithm (base 10) of the distance between the ith shotpoint and the jth trace location, (in units of km),

w_i is the logarithm (base 10) of the charge size (weight) of the ith shot, (in units of kg), and

b_1, b_2, c_1, g_X are constants to be inverted for.

g_X is a constant for ground conditions, which govern the efficiency of shot coupling.

Four ground conditions were recognized: 1. wet alluvium (g_A), 2. dry alluvium (g_D), 3. bedrock (g_R), and 4. sedimentary rocks (g_S). "Wet alluvium" and "dry alluvium" apply to all Quaternary and Pliocene/Quaternary deposits which have some or no standing water, respectively, in shotholes prior to loading. "Bedrock" applies to Mesozoic and older rocks, and "sedimentary rocks" applies to Tertiary sedimentary rocks. a_{ij}, x_{ij}, and w_i are known, and b_1, b_2, c_1, and g_1 are unknowns.

The data in Fig. 8 can be fitted with two different curves, with approximately similar standard errors, depending on whether the (a_{ij}, x_{ij}) points are weighted by distance (1/x) or not. The model curve shown in Fig. 8 is for distance weighting, which, of course, emphasizes data at small distances:

For 1/x distance weighting:

variable	value	std dev
b_1	-1.9277	0.0053 distance factor
b_2	-0.3411	0.0037 distance-squared factor
c_1	0.8119	0.0245 charge-size factor
g_R	-3.0059	0.0137 correction for bedrock sites
g_A	-3.1249	0.0366 correction for wet alluvium sites
g_D	-3.5600	0.0395 correction for dry alluvium sites
g_S	-3.8767	0.0801 correction for sedimentary-rock sites

Number of points 2163

Standard error 0.57 (in units of $\log_{10}$ cm/s)

For no distance weighting:

b_1	-1.6068	0.0549 distance factor
b_2	0.0190	0.0738 distance-squared factor
c_1	0.8022	0.0235 charge-size factor
g_R	-3.2789	0.0127 correction for bedrock sites
g_A	-3.3791	0.0364 correction for wet alluvium sites
g_D	-3.8278	0.0391 correction for dry alluvium sites
g_S	-4.1457	0.0796 correction for sedimentary-rock sites

Number of points 2164
Standard error 0.55

In Fig. 8, the model curve and data move up or down depending on which shot size and site constants g are used to correct the data. Additional curves can be plotted to bracket 90% or 99% of the data. (In Fig. 8, the 99% curve--approximately 2 standard deviations above the model curve--is shown.) The intersections of these latter curves with 3 different thresholds of concern determine shot size. The thresholds are ~ 2.5 cm/s (1 in/s) (at frequencies less than 40 Hz) for human complaints, ~5 cm/s (2 in/s) for incipient damage to old stucco, and 12.5 cm/s (5 in/s) for potential damage to older engineered structures (Edwards and Northwood, 1960; Nicholls and others, 1971; Blasters' Handbook, 1977; Northwood and others, 1963; Stagg, and others, 1980; W. Bender, written manual "Explosives Training Course", 1992)., We most commonly used the 99% curve to avoid human complaints and potential cosmetic damage to private residences, and the 90% curve to avoid potential damage to engineered structures. To easily determine shot size, we constructed two tables listing shot size and distance (a) for various shotpoint site factors, (b) for 90% and 99% certainty, and (c) for the 3 thresholds above (APPENDIX I). One table was constructed using a model curve determined with distance weighting (1/x) (APPENDIX Ia) and another, with no distance weighting (APPENDIX Ib). The final shot size determined for a particular location was an average of values from these 2 tables.

The procedure outlined above was quite successful in avoiding human complaints and structure damage. The occurrence of the Hector Mine earthquake 4 days before shooting began, may, however, have been a factor in reducing human complaints, as aftershocks continued to be felt for days after the earthquake. Fortunately, these aftershocks did not seriously contaminate the explosion data.

To aid in the planning of future seismic surveys of the LARSE type, we have used LARSE II data to determine how far P-waves will propagate for a given shot size (Fig. 9; Table 2b). P-wave propagation distances were picked, where they did not extend to (and presumably beyond) the ends of the main line. P-wave arrivals at the picked distances were required to have discernable upward first motion. We did not distinguish shotpoint site conditions/geology in Fig. 9, although such a grouping could be done based on the column headed "Geologic site label." in Table 2b (see discussion above). We also picked distances to which energy of any type was discernable from each shotpoint (Table 2b).

The data obtained in LARSE II are displayed in Murphy and others (in preparation), and examples are given in Figs. 10-13. With the exception of data from a couple of shotpoints, data quality is fair to excellent. We were generally quite pleased with both the propagation distances for seismic energy and with signal-to-noise ratios, especially along urbanized sections of our various lines. Data quality appears higher, for example, in the San Fernando Valley than was our experience in the San Gabriel Valley on LARSE Line 1. Further analysis of the data will be required to make more quantitative statements, however. We had some truly exceptional energy propagation from some of our small shots in the San Fernando Valley (see Figs. 11, 12).

SEISMIC ACQUISITION SYSTEMS

Five different types of seismograph systems were used to acquire seismic data during LARSE II: PRS1's and PRS4's (developed by the Geological Survey of Canada), SGR III's (developed by Globe Universal Sciences, Inc., for AMOCO), RefTeks (developed by Refraction Technology for IRIS/PASSCAL), Texans (developed by Refraction Technology for University of Texas, El Paso, and IRIS/PASSCAL), and PDAS (developed by Teledyne/Geotech) (Table 1). A general description of each is given in Murphy and others (in preparation), but for more detailed descriptions of RefTeks and Texans, see the IRIS/PASSCAL web site (http://www.passcal.nmt.edu). For the PRS1's and PRS4's, see Asudeh and others (1992), and for the SGR III's, see the technical manual by Globe Universal Sciences, Inc. and the L-10 geophone specifications by Mark Products. No general references are available for the PDAS's.

EXPERIMENT SCHEDULE

The LARSE II field work began in mid-June 1999 with shothole drilling. Drilling was stopped in mid-July due to the slow pace of permitting and resumed in September. It continued until October 22, our 3rd day of shooting. In August, several survey parties began staking, flagging, and logging recorder sites. In urban and suburban areas, where many recorder sites had to be located on private property, survey parties had to do intensive permitting as well. Calibration shots were drilled and loaded in early September, and detonated on September 17. Loading of shot holes for the main survey began on October 4 and continued through October 24. In mid-October, seismic recording systems and personnel were assembled from numerous institutions. Instrumentation was tested and instruments were deployed over a three day period starting October 17. Instruments with the longest battery lives (Refteks, PRS1's, PRS4's, SGR's and PDAS's) were deployed in the first 2 days and instruments with the shortest battery lives (Texans) deployed on October 19. Sixty two shots were detonated on October 20-22 (Julian days 293-295--see Table 2a) by a maximum of 11 shooting teams/night, each shooting 1 minute apart during 11-minute intervals beginning at 1:30 AM, 3:00 AM, and 4:30 AM. Thirty-one shots in the City of Los Angeles were loaded on October 23 and detonated on October 24-25 (Julian days 297-298--see Table 2a) during the same early-morning time intervals as above. Cleanup of Los Angeles City shotpoints began on October 24, and cleanup of the entire survey was completed by the mid-November. Data processing and cleanup began in November and continued until October 2000, when it was made available on the SCEC web site to LARSE researchers.

DETERMING LOCATIONS

Horizontal locations for both shotpoints and recorders were obtained using a Global Positioning Satellite navigation system (GPS). Accuracy is estimated to be 3-5 m. Vertical locations (elevations) were obtained by an alternative method, as some GPS elevations were either not reported or were highly inaccurate. In this method, horizontal locations were used to extract elevations from 10-m Digital Elevation Models (DEM's). These have estimated average errors in hilly terrain of ~6 m, and less in flat terrain. The range of error is probably 5-10 m. Horizontal locations of shotpoints, both Latitude/Longitude and Universal Transverse Mercator (UTM) projections for Zone 11, are given in Table 2a with respect to the WGS84/NAD83 datum. Elevations are given with respect to Mean Sea Level (MSL). Recorder locations and elevations are given in Murphy and others (in preparation).

DATA PROCESSING

The mix of instruments posed several unique recording problems. The PRS1's and PRS4's have an instrument response designed for lower-frequency refraction/wide-angle reflection recording (2-20 Hz), whereas the SGRs, RefTeks, Texans, and PDAS's are designed for higher-frequency reflection recording. Although all of the playback systems produce SEG-Y data tapes, the header files and sample rates are different for each system. Merging the data required extensive processing, as follows:

Data Reduction and Merging

Seismograms from the diverse types of instrumentation were combined to form complete common shot gathers. This data merging was performed to archive the data using proper SEG-Y formatting but in a manner which would be useful for subsequent data analysis. The SEG-Y standard requires that all the data have common sampling rates and lengths with coherent indexing within the SEG-Y trace headers.

The archival data was primarily organized by seismic array (Lines 2, 3000, 4000, 5000, 6000, 7000, and the scatter array "6A"). Each array collected all 93 explosion sources. The number of instruments per array varied as did the number of 3-component versus single component instruments; as a result, the number of total seismic traces in an array's shot gather is varied. These values are summarized:

Line	Stations	#stations	#shots	#traces per shot
2	1001-2500	954	93	1296
3000	3001-3058	56	93	82
4000	4006-4114	81	93	117
5000	5010-5073	30	93	34
6000	6005-6108	90	93	134
7000	7001-7063	54	93	64
6A	6503-6557	49	93	147

A description of which instrument type was deployed at which station is provided in Murphy and others (in preparation). The data were organized by line. Within each line, data were ordered primarily by shot and secondarily by "channel". Channel number is based on station location and on station components. Channel numbering starts in the south at the ocean and is increased northward by each trace. Each 1-component station increases the number by one and each 3-component station increases the number by three. For example a Texan adds one trace to the channel number and a RefTek adds three traces to the channel number.

Data merging was performed using a software application which was written specifically for merging the LARSE data. This application used lists to place seismograms in low-to-high station location order for each array. Prior to ordering, the application program performed procedures common to all the data and made several adjustments to the data based on instrument type.

The incoming data had the following characteristics:

Inst type (DAS)	#samples per trace	sample interval	#sec	time of first sample (sec)
PRS-1	3841	1/120.	32	-2.000
PRS-4	3841	1/120	32	-2.000
SGR	15501	.002	31	-1.000

Reftek	15500	.004	62	-1.996
PDAS	12401	.005	62	-2.000
Reftek Texan	11250	.004	45	-0.996

The final data had the following characteristics:

Inst type (DAS)	#samples per trace	sample interval	#sec	time of first sample (sec)
All instruments	15501	.004	62	-2.00

The following procedures were performed on data from each instrument type prior to merging:

PRS1 and PRS4:

a) amplitude debias.
b) static time shift based on preprocessing trace header value
- due to DAS programming.
c) hand static and shot static
(described in "Quality Assurance" section below).
d) convert *PRS1/4* sampling rate to archival sampling rate
using cubic spline interpolation of each seismogram.
e) zero-pad seismograms to desired output trace length.

SGR:

a) amplitude debias.
b) hand static and shot static
(described in "Quality Assurance" section below).
c) convert SGR sampling rate to archival sampling rate
using cubic spline interpolation of each seismogram.
d) zero-pad seismograms to desired output trace length.

Reftek:

a) amplitude debias.
b) hand static and shot static
(described in "Quality Assurance" section below).
c) polarity reversal.
d) zero-pad seismograms to desired output trace length.

PDAS:

a) amplitude debias.
b) hand static and shot static
(described in "Quality Assurance" section below).
c) convert PDAS sampling rate to archival sampling rate
using cubic spline interpolation of each seismogram.
d) zero-pad seismograms to desired output trace length.

Texan:

a) amplitude debias.
b) hand static and shot static (see below)
(described in "Quality Assurance" section below).
c) polarity reversal.
d) zero-pad seismograms to desired output trace length.

Upon merging, appropriate index trace headers were assigned, where order within a line was based primarily on shot number and secondarily on station location. Additional trace headers were also defined such as latitude/longitude and UTM coordinates, offset distances, field geometries and data descriptions (see Murphy and others, in preparation).

A preliminary version of merged data was produced in April 2000. These data were visually inspected by LARSE personnel at the USGS. Individual seismogram corrections were identified primarily in regards to first arrival travel time (hand static) and polarity reversals. These corrections were applied upon final archive-quality merging. Several shots required bulk time shifts (shot static) due to their shot initiation times being delayed from the desired shot time (which were "on-the-minute").

Quality Assurance

The data were displayed in record sections reduced by 6 km/s. Each trace was examined for potential problems with timing, polarity, and location.

Timing: For traces whose first-arrivals were consistently out of line with adjacent traces by more than ~40-50 ms, the time difference was recorded for each shot (see for example Table 4a). Time differences for each trace for each 11-minute shot window were averaged (see, for example, Table 4b). Numerical flags were defined and attached to each timing correction according to the size of the correction and to its certainty. To further investigate these timing problems for the Refteks, where independent timing information is available, we examined internal instrument logs. All but one of the 23 Refteks with initial tabulated timing corrections, as identified by visual timing misalignment, had evidence in their internal logs indicating timing problems. (Timing corrections for the single Reftek without independent evidence of timing problems were deleted.)

Polarity: For traces with impulsive first arrivals, polarity reversals were noted (Table 4a) and a flag was set in Table 4b to correct the polarity.

Location: A few traces had timing problems that were interpretable as location or duplication problems. These problems were noted (Table 4a) and flagged (Table 4b).

The timing, polarity, and location/duplication corrections were applied to the data, and these corrections and accompanying flags were written to the SEG-Y trace headers so that future researchers can undo the corrections if desired.

WATER LEVELS IN SHOTHOLES

Information on the water table is generally of immediate use to shotpoint permittors (Table 2b; Fig.14). "Water table" is a simplified concept wherein the upper part of the Earth's crust is thought of as a porous medium with water existing uniformly in the pores below a horizon, the "water table", that generally varies laterally in a smooth fashion. Permanent streams would represent "outcrops" of the water table, and intermittent streams would represent "outcrops" of the water table when it is high enough to intersect the bottoms of valleys. Lakes may represent a "perched water table" with an impervious layer of rock or soil beneath it, separating it from the main "water table" below. Porosity occurs as both voids between the various grains and minerals that make up rock or as cracks and fault zones. Generally, cracks are present in the upper few km of the Earth's crust, but they close as pressure gets higher with depth. Active fault zones provide porosity to much greater depths than in surrounding rock. In the real Earth, porosity may vary drastically from one body of rock to the next, and these rock bodies do not necessarily form simple layers in the Earth. Thus, one may find that there are dramatic differences in water level from well to well, even when the wells are closely spaced.

In examining a profile of water levels along the main LARSE Line 2 (Fig.14), one sees some wells that obey the simple concept of a "water table" and others that do not. For example SP's 8020-8045 (Table 2b; Fig. 14, numbers 1-4) are located along intermittent streams in the southern Santa Monica Mountains, and reflect a shallow water table that is near the surface. A similar observation is also made for SP's 8120-8210 (Table 2b; Fig. 14, numbers 14-19), which span the Los Angles River (located near number 17), SP's 8490-8502 (Table 2b; Fig. 14, numbers 42-44), located in a large desert wash on the south flank of Sierra Pelona, and SP's 8700 and 8720 (Table 2b; Fig. 14, numbers 60, 62), located in intermittent washes in or near the San Andreas fault zone. A striking exception to the simple "water table" concept is SP 8590 (Table 2b; Fig. 14, number 51), located in the large wash of San Francisquito Canyon and near (but not in) the inactive San Francisquito fault zone (Fig. 4). This shotpoint was drilled into the almost impermeable Pelona Schist. Immediately to the south, SP's 8540-8570 apparently represent a "perched water table" atop the Sierra Pelona (Table 2b; Fig.14, numbers 48-50). These shotpoints are also drilled into Pelona Schist, but at these locations, apparently the upper part of the Pelona Schist is permeable. One additional example of a "perched water table" is SP 8270 (Table 2b; Fig. 14, number 25), in the dry northern San Fernando Valley; this shotpoint is located in a local debris basin/lake. One notes that water level in the central Santa Monica Mountains, Santa Susana Mountains, Santa Clarita Valley, central Transverse Ranges, Mojave Desert, and Sierra Nevada is generally deeper than along other parts of the line (greater than 24 m, or 80 ft). These greater depths may result from any or all of the following factors: 1) greater distance from and elevation above streams, 2) poorly permeable bedrock, and 3) rainfall deficit compared to adjacent areas.

ACKNOWLEDGMENTS

LARSE II was a difficult survey to permit, deploy, shoot, and cleanup. We had welcome help from many government agencies, institutions, and individuals. In Table 5, we list these agencies, institutions, and key individuals who made this survey possible. We would like to mention especially the following: The U.S. Forest Service (Saugus District) and Mike Wickman gave a swift and thorough review of our environmental assessment and streamlined the permitting process. The staff of the City of Los Angeles expedited our permitting process at a cost of approximately $25,000, born by the City. Mike Michalski and Linda Moore helped us scout for shotpoints on City property; Andy Gutierrez oversaw and assisted us with safety compliance for our explosions; and Mark Mackowski and Simon Hsu were helpful in our permitting process along the Los Angeles aqueduct. Rich Rozelle, Randy Cedarquist, and Jeff Bolton expedited our permitting process for Topanga State Park and for surrounding lands under the jurisdiction of the Santa Monica Mountains Conservancy. Tom Tindall and his staff guided us in getting permission from California State University at Northridge; John Chandler influenced the content of our LARSE "Fact Sheet" (Henyey and others, 1999a). Evan Morris (Los Angeles Unified School District), Evan Aldrich (City of Santa Clarita), Mike Otavka (W.S. Hart School District), and Mark Fulmer (Saugus Elementary School District) assisted us in getting permission for shotpoints on school properties. Karvel Bass coordinated our permit process with the U.S. Army Corps of Engineers, and Teresa Castillo signed our permit from the U.S. Veterans Administration. Robert Sagehorn (Castaic Lake Water Agency), assisted by Michael Thompson, kindly gave us permission for shotpoints and access to Water Agency land. Peter Sego, Tom Shroeder, Jim Mansdorfer, and Sharon O'Rouke were helpful in our obtaining permits from the Southern California Gas Company. Ralph Herman, owner of El Caballero Country Club and former owner of much of the land surrounding the south end of Reseda Blvd in Tarzana, kindly assisted us in finding shotpoints in that area. Paul Ramina and Gerd Koenig were helpful in our obtaining a permit from Riviera Country Club. Joan Akins (City of Santa Monica), Councilperson Cindy Miscikowski (City of Los Angeles), and Lisa Merlino (City of Los Angeles) were instrumental in our obtaining permits for a vibrating truck in the Santa Monica area (see Baher and others, in review, for a description of the vibroseis survey). Steven Seemann (Richmond American Homes) and Bruce Harrigan (Playa Vista Development Company) were the only land developers to give us permits; we were grateful. James Aidukas and James Ambroso (BFI Sunshine Canyon Landfill) gave us permits for key shotpoints in the Santa Susana Mountains. Dana Stewart (The Oaks Camp and Conference Center) was the first to sign any of our LARSE permit requests, giving us initial encouragement. Byron McMichael (National Cement Company) gave us an important shotpoint in the Tehachapi Mountains. George Jackman allowed us to store explosives in his "Magazine Canyon" compound. Finally, numerous private land owners all along the LARSE lines gave us permission for shotpoint and seismograph locations; thirty-two gave permission for shotpoints (Table 5).

The personnel needed to carry out this experiment, 123 in number, were provided by a large group of universities, organizations, and private companies (APPENDIX II). Even with this large number of people, we were understaffed, and everyone was forced to work long hours. As a credit to this enormous collective effort, LARSE II was successful.

Our two contractors, Sam Crum (Sam Crum Water Well Drilling) and Gordon Coleman (Alpha Explosives), worked as part of the LARSE team. Without their expert and willing efforts, we would have no seismic results to report.

Finally, we would like to thank Jim Luetgert for reviewing this report.

REFERENCES CITED

(For additional LARSE publications, reports, abstracts, and videos see APPENDIX III)

Allen C. R., Engen, G. R., Hanks, T. C., Nordquist, J. M., and Thatcher, W. R., 1971, Main Shock and larger aftershocks of the San Fernando earthquake, February 9 through March 1, 1971, in *The San Fernando, California, Earthquake of February 9, 1971*: U.S. Geological Survey Professional Paper 733, p. 17-20.

Allen C. R., Hanks, T. C., and Whitcomb, J. H., 1975, Seismological studies of the San Fernando earthquake and their tectonic implications, in *San Fernando, California, Earthquake of 9 February 1971*, edited by G. B. Oakeshott: California Division of Mines and Geology Bulletin 196, p. 257-262.

Asudeh, I., Anderson, F., Parmelee, J., Vishnubhatla, S., Munro, P., and Thomas, J., 1992, A portable refraction seismograph PRS1: Geological Survey of Canada Open-file Report 2478, 34 p.

Baher, S., Davis, P., Clayton, R., and Fuis, G., Seismic Reflection Data Acquired in the Los Angeles Region Seismic Experiment (LARSE II), Los Angeles, California, using Vibroseis Sources: U.S. Geological Survey Open-File Report (in preparation),

Bohannon, R.G., 1975, Mid-Tertiary conglomerates and their bearing on Transverse Range tectonics, southern California, in *The San Andreas Fault in Southern California,* edited by J.C. Crowell: California Division of Mines and Geology Special Report 118, p. 75-82.

Brocher, T.M., Clayton, R.W., Klitgord, K.D., Bohannon, R.G., Sliter, R., McRaney, J.K., Gardner, J.V., and Keene, J.B., 1995, Multichannel seismic-reflection profiling on the R/V Maurice Ewing during the Los Angeles Region Seismic Experiment (LARSE), California: U.S. Geological Survey Open File Report 95-228, 70 p.

Campbell, R.H., Yerkes, R.F., and Wentworth, C.M., 1966, Detachment Faults in the Central Santa Monica Mountains, California, in *Geological Survey Research 1966*: U.S. Geological Survey Professional Paper 550-C, p. C1-C11.

Crouch, J.K., and Suppe, J., 1993, Late Cenozoic evolution of the Los Angeles basin and inner California borderland: A model for core complex-like crustal extention: Geological Society of America Bulletin, v. 105, p. 1415-1434.

Crowell, J. C., 1954, Strike-slip displacement of the San Gabriel fault, southern California, in *Geology of Southern California*, edited by R. H. Jahns: California Division of Mines Bulletin 170, Chapter IV: Structural Features, v 1, p. 49-52.

Crowell, J.C., 1962, Displacement along the San Andreas fault, California: Geological Society of America Special Paper 71, 61 p.

Crowell, J.C., 1982, The tectonics of the Ridge basin, southern California, in *Geologic History of the Ridge Basin, Southern California*, edited by J.C. Crowell, and M.H. Link: Pacific Section, Society of Economic Paleontologists and Mineralogists, p. 25-42.

Davis, P.M., Rubenstein, J.L., Liu, K.H., Gao, S.S., Knopoff, L., 2000, Northridge earthquake damage caused by geologic focussing of seismic waves: Science, v. 289, p. 1746-1750.

Dibblee, T.W., Jr., 1967, Areal geology of the western Mojave Desert, California: U.S. Geological Survey Professional Paper 522, 153 p.

Dibblee, T.W., Jr., 1992, Geologic map of the Topanga and Canoga Park (south 1/2) quadrangles, Los Angeles County, California: Santa Barbara, Calif., Dibblee Geological Foundation, scale 1:24,000.

Dibblee, T.W., Jr., 1996, Geologic map of the Newhall quadrangle, Los Angeles County, California: Santa Barbara, Calif., Dibblee Geological Foundation, scale 1:24,000.

Ehlig, P. L., 1968, Causes of distribution of Pelona, Rand and Orocopia schists along the San Andreas and Garlock faults, in *Proceedings of Conference on Geologic Problems of San Andreas Fault System*, edited by W.R. Dickinson, and A. Grantz: Stanford University Publications, Stanford, California, p. 294-306.

Ehlig, P. L., 1981, Origin and tectonic history of the basement terrane of the San Gabriel Mountains, central Transverse Ranges, in *The Geotectonic Development of California,* edited by W.G. Ernst: Prentice-Hall, Englewood Cliffs, New Jersey, p. 253-283,

Ehlig, P.L., Ehlert, K.W., and Crowe, B.M., 1975, Offset of the upper Miocene Caliente and Mint Canyon formations along the San Gabriel and San Andreas faults, in *The San Andreas Fault in Southern California*, edited by J.C. Crowell: California Division of Mines and Geology Special Report 118, p. 83-92.

Field, N., Jones, L., and Jordan, T., 2001, Earthquake shaking--Finding the "hotspots": U.S. Geological Survey Fact Sheet 001-01.

Fuis, G.S., Ryberg, T., Godfrey, N.J., Okaya, D.A., and Murphy, J.M., 2001, Crustal structure and tectonics from the Los Angeles basin to the Mojave Desert, southern California: Geology, v. 29, p. 15-18.

Gao, S., Liu, H., Davis, P.M., and Knopoff, L., 1996, Localized amplification of seismic waves and correlation with damage due to the Northridge earthquake: Bulletin of the Seismological Society of America, v. 86, p. 209-230.

Hauksson, E., Jones, L. M., and Hutton, K., 1995, The 1994 Northridge earthquake sequence in California: Seismological and tectonic aspects: Journal of Geophysical Research, v. 100, p.12,335-12,355.

Henyey, T.L., Fuis, G.S., Benthien, M.L., Burdette, T.R., Christofferson, S.A., Clayton, R.W., Criley, E.E., Davis, P.M., Hendley, J.W., II, Kohler, M.D., Lutter, W.J., McRaney, J.K., Murphy, J.M., Okaya, D.A., Ryberg, T., Simila, G., and Stauffer, P.H., 1999a, The "LARSE" Project--working toward a safer future for Los Angeles, U.S. Geological Survey Fact Sheet 110-99, 2 p.

Henyey, T.L., Fuis, G.S., Anima, R.J., Barrales-Santillo, A., Benthien, M.L., Burdette, T.R., Christofferson, S.A., Criley, E.E., Clayton, R.W., Davis, P.M., Garcia, S., Hendley, J.W., II, Kohler, M.D., Lutter, W.J., McRaney, J.K., Murphy, J.M., Okaya, D.A., Ryberg, T., Simila, G., y Stauffer, P.H., 1999b, El proyecto sísmico "LARSE"--Trabajando hacia un futuro con mas seguridad para Los Angeles, U.S. Geological Survey Fact Sheet 111-99.

Hornafius, J.S., Luyendyk, B.P., Terres, R.R., and Kamerling, M.J., 1986, Timing and extent of Neogene tectonic rotation in the western Transverse Ranges, California: Geological Society of America Bulletin, v. 97, p. 1476-1487.

Jahns, R.H., and Muehlberger, W.R., 1954, Geology of Soledad basin, Los Angeles County, in *Geology of Southern California*, edited by R. H. Jahns: California Division of Mines Bulletin 170, v 2, Map sheet no. 6.

Jennings, C.W., compiler, 1977, Geologic map of California: California Division of Mines and Geology, scale 1:750,000.

Jennings, C. W., and Strand, R. G., 1969, Geologic map of California, Los Angeles sheet: California Division of Mines and Geology, scale 1:250,000.

Heaton, T.H., 1982, The 1971 San Fernando earthquake: a double event?: Bulletin of Seismological Society of America: v. 72, p. 2037-2062.

Kohler, M.D., Davis, P.M., Liu, H., Benthien, M., Gao, S., Fuis, G.S., Clayton, R.W., Okaya, D., and Mori, J., 1996, Data report for the 1993 Los Angeles Region Seismic Experiment (LARSE 93), southern California: a passive study from Seal Beach northeastward through the Mojave Desert: U.S. Geological Survey Open-File Report 96-85, 82 p.

Kohler, M. D., and Kerr, B. C., Data report for the 1998-1999 Los Angeles Region Seismic Experiment II Passive Array: U.S. Geological Survey Open-File Report (in preparation),

Kohler, M.D., Kerr, B.C., and Davis, P.M., 2000, The 1997 Los Angeles basin passive seismic experiment--a dense, urban seismic array to investigate basin lithospheric structures: U.S. Geological Survey Open-File Report 00-148, 109 pp.

Kohler, W. M., and Fuis, G. S., 1992, Empirical relationship among shot size, shotpoint site condition, and recording distance for 1984-1987 U.S. Geological Survey seismic-refraction data: USGS Open-File Report 89-675, 107 p.

Langenheim, V.E., Griscom, A., Jachens, R.C., and Hildenbrand, T.G., 2000, Preliminary potential field constraints on the geometry of the San Fernando basin, southern California: U.S. Geological Survey Open-File Report 00-219, 17 p.

Matti, J.C., Morton, D.M., and Cox, B.F., 1985, Distribution and geologic relations of fault systems in the vicinity of the central Transverse Ranges, southern California: U.S. Geological Survey Open-File Report 85-365, 27 p. scale 1:250,000.

McCulloh, T.H., Beyer, L.A., and Enrico. R.J., 2000, Paleogene Strata of the eastern Los Angeles basin, California: Paleogeography and constraints on Neogene structural evolution: Geological Society of America Bulletin, v. 112, p. 1155-1178.

Meisling, K. E., and Weldon, R. J., 1989, Late Cenozoic tectonics of the northwestern San Bernardino Mountains, southern California: Geological Society of America Bulletin, v. 101, p. 106-128.

Mori, J., Wald, D.J., and Wesson, R.L., 1995, Overlapping fault planes of the 1971 San Fernando and 1994 Northridge, California earthquakes: Geophysical Research Letters, v 22, p. 1033-1036.

Murphy, J. M., Fuis, G. S., Okaya, D.A., Thygesen, K., Baher, S.A., Kaip, G., Fort, M.D., Asudeh, I., Report for borehole explosion data acquired in the 1999 Los Angeles Region Seismic Experiment (LARSE II), Southern California: Part II DATA: U.S. Geological Survey Open-File Report (in preparation),

Murphy, J.M., Fuis, G.S., Ryberg, T., Okaya, D.A., Criley, E.E., Benthien, M.L., Alvarez, M., Asudeh, I., Kohler, W.M., Glassmoyer, G.N., Robertson, M.C., and Bhowmik, J., 1996, Report for explosion data acquired in the 1994 Los Angeles Region Seismic Experiment (LARSE94), Los Angeles, California: U.S. Geological Survey Open-File Report 96-536, 120 p.

Oakeshott, G.B., 1975, Geology of the Epicentral Area, in *San Fernando, California, Earthquake of 9 February 1971*, edited by G. B. Oakeshott: California Division of Mines and Geology Bulletin 196, pp. 1-30.

Okaya, D.A., Bhowmik, J., Fuis, G.S., Murphy, J.M., Robertson, M.C., Chakraborty, A., Benthien, M.L., Hafner, K., and Norris, J.J., 1996a, Report for air-gun data acquired at onshore stations during the 1994 Los Angeles Region Seismic Experiment (LARSE), California: U.S. Geological Survey Open-File Report 96-297, 224 p.

Okaya, D.A., Bhowmik, J., Fuis, G.S., Murphy, J.M., Robertson, M.C., Chakraborty, A., Benthien, M.L., Hafner, K., and Norris, J.J.,1996b, Report for local earthquake data acquired at onshore stations during the 1994 Los Angeles Region Seismic Experiment (LARSE), California: U.S. Geological Survey Open-File Report 96-509, 332 p.

Oliver H.W., Chapman, R.H., Biehler, S., Robbins, S.L., Hanna, W.F., Griscom, A.,. Beyer, L.A., Silver, E.A., 1980, Gravity map of California, and it's continental margin: California Division of Mines and Geology Geologic Data Map No. 3., scale 1:750,000.

Powell, R. E., Balanced palinspastic reconstruction of pre-late Cenozoic paleogeology, southern California: Geologic and kinematic constraints on evolution of the San Andreas fault system, 1993, in *The San Andreas Fault System: Displacement, Palinspastic Reconstruction, and Geologic Evolution,* edited by R.R. Powell, R.J. Weldon, and J.C. Matti: Geological Society of America Memoir 178 , p. 1-106.

Stitt, L.T., 1986, Structural history of the San Gabriel fault and other Neogene structures of the central Transverse Ranges, in *Neotectonics and Faulting in Southern California,* compiled by P.L. Ehlig: Geological Society of America, 82nd Annual Meeting of Cordilleran Section, Guidebook and Volume for Field Trips 10, 12, 18, p. 43-102.

ten Brink, U.S., Drury, R.M., Miller, G.K., Brocher, T. M., and Okaya, D.A., 1996, Los Angeles Region Seismic Experiment (LARSE), California off-shore seismic refraction data: USGS Open-File Report 96-27, 29 p.

Tsutsumi, H., and Yeats, R.S., 1999, Tectonic setting of the 1971 Sylmar and 1994 Northridge earthquakes in the San Fernando Valley, California: Bulletin of Seismological Society of America, v. 89, p.1232-1249.

U.S. Geological Survey staff, 1971, Surface Faulting, , in *The San Fernando, California, Earthquake of February 9, 1971:* U.S. Geological Survey Professional Paper 733, pp. 55-76.

Wald, D.J., and Graves, R.W., 1998, The seismic response of the Los Angeles Basin, California: Seismological Society of America Bulletin, v. 88, p. 337-356.

Weber, F. H., Jr., 1975, Surface Effects and Related Geology of the San Fernando Earthquake in the Sylmar Area, in *San Fernando, California, Earthquake of 9 February 1971*, edited by G. B. Oakeshott: California Division of Mines and Geology Bulletin 196, pp. 70-96.

Winterer, E.L., and Durham, D.L., 1954, , Geology of a part of the eastern Ventura basin, Los Angeles county, in *Geology of Southern California*, edited by R. H. Jahns: California Division of Mines Bulletin 170, v 2, Map sheet no. 5

Working Group on California Earthquake Probabilities, 1995, Seismic hazards in southern California: Probable earthquakes, 1994-2024: Seismological Society of America Bulletin, v. 85, p. 379-439.

Wright, T.L., 1991, Structural geology and tectonic evolution of the Los Angeles basin, California, in *Active Margin Basins,* edited by K.T. Biddle: American Association of Petroleum Geologists Memoir 52, p. 35-134.

Yeats, R.F., 1987, Late Cenozoic structure of the Santa Susana fault zone, in *Recent Reverse Faulting in the Transverse Ranges, California*: U.S. Geological Survey Professional Paper 1339, 137-160.

Yeats, R.S., Huftile, G.J., and Stitt, L.T.,1994, Late Cenozoic tectonics of the east Ventura basin, Transverse Ranges, California: American Association of Petroleum Geologists Bulletin, v. 78, pp 1040-1074.

Yerkes, R.F., and Campbell, R.H., 1980, Geologic Map of east-central Santa Monica Mountains, Los Angeles County, California: U.S. Geological Survey Miscellaneous Investigation Series, Map I-1146, scale 1:24,000.

Yerkes, R.F., McCulloh, T.H., Schoellhamer, J.E., and Vedder, J.G., 1965, Geology of the Los Angeles basin, California--An introduction: U.S. Geological Survey Professional Paper 420-A, 57 p.

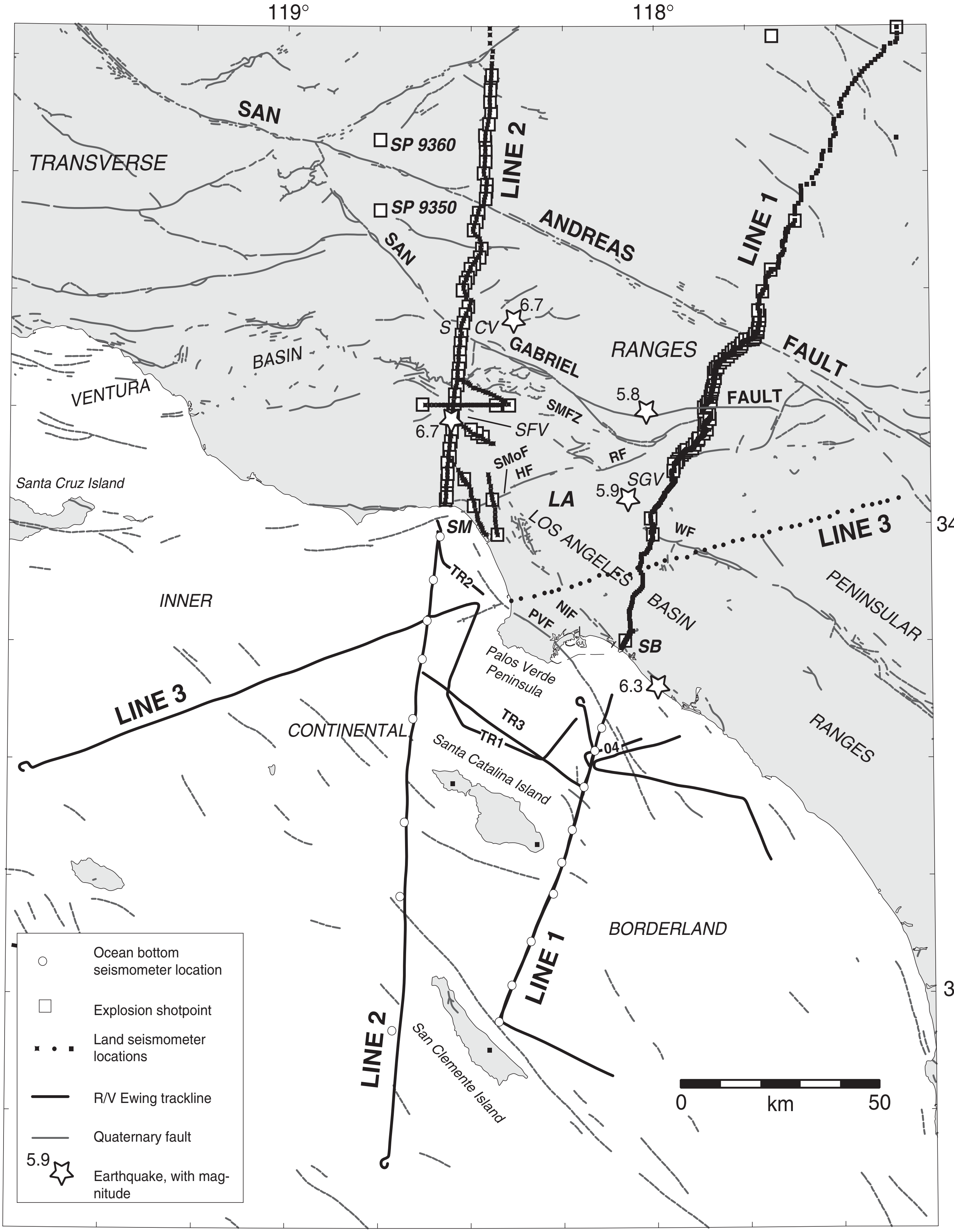

Figure 1. Fault map of Los Angeles region showing LARSE lines. Abbreviations: HF, Hollywood fault; LA, Los Angeles; NIF, Newport-Inglewood fault; PVF, Palos Verde fault; RF, Raymond fault; SB, Seal Beach; SCV, Santa Clarita Valley; SFV. San Fernando Valley; SGV, San Gabriel Valley; SM, Santa Monica; SMFZ, Sierra Madre fault zone; SMoF, Santa Monica fault; TR1-4, transit lines 1-4; WF, Whittier fault.

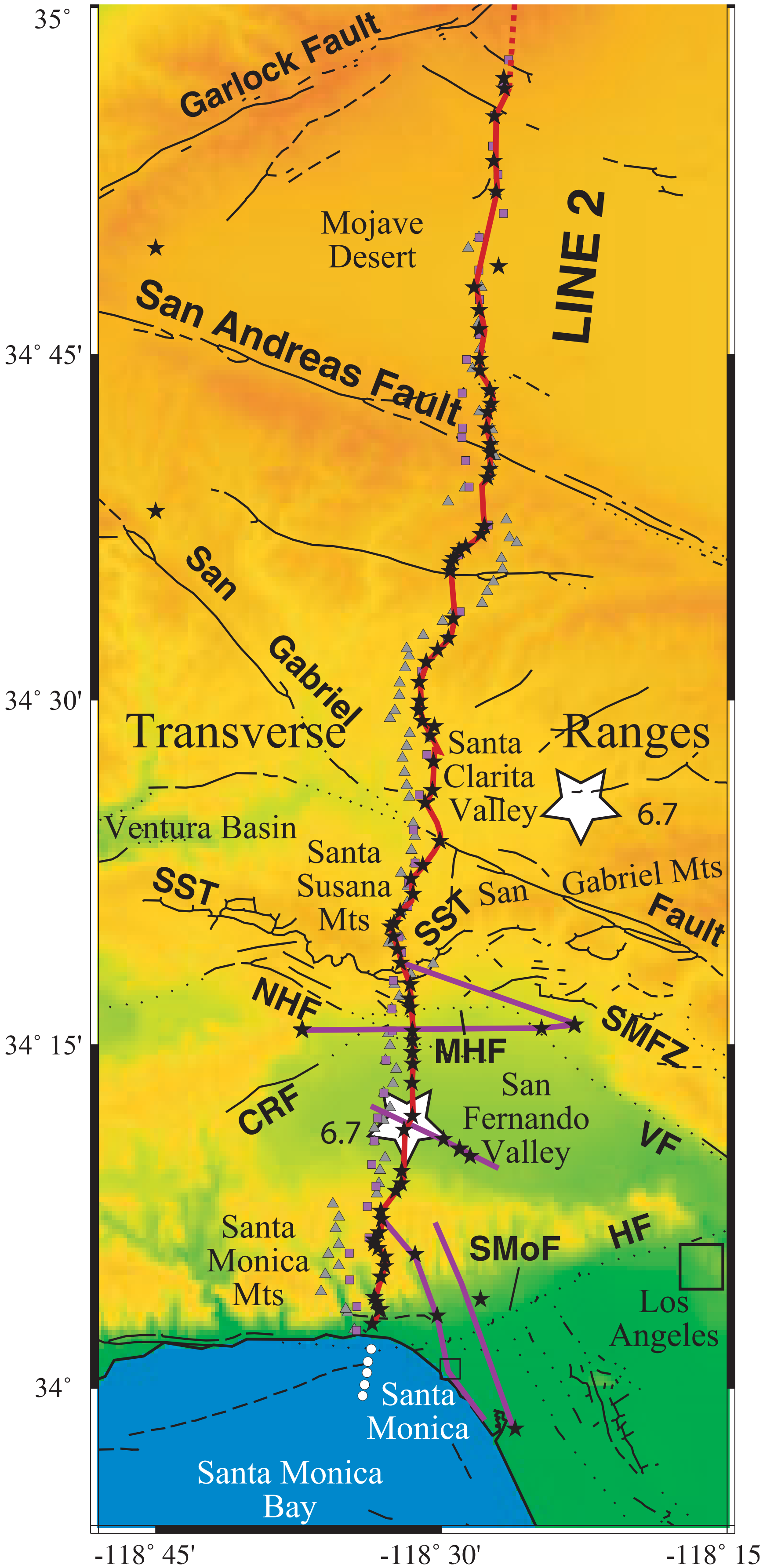

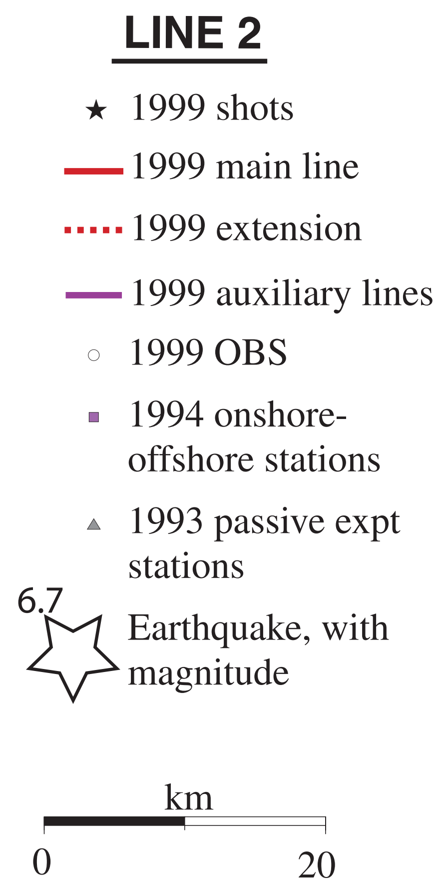

Figure 2. Fault map of northwestern part of the Los Angeles region showing shotpoint and seismograph locations along LARSE Line 2. Faults are abbreviated as in Fig. 1 with additions, CRF-Chatsworth Reservoir fault, MHF-Mission Hills fault, NHF-Northridge Hills fault, SST-Santa Susana thrust fault, and VF-Verdugo fault.

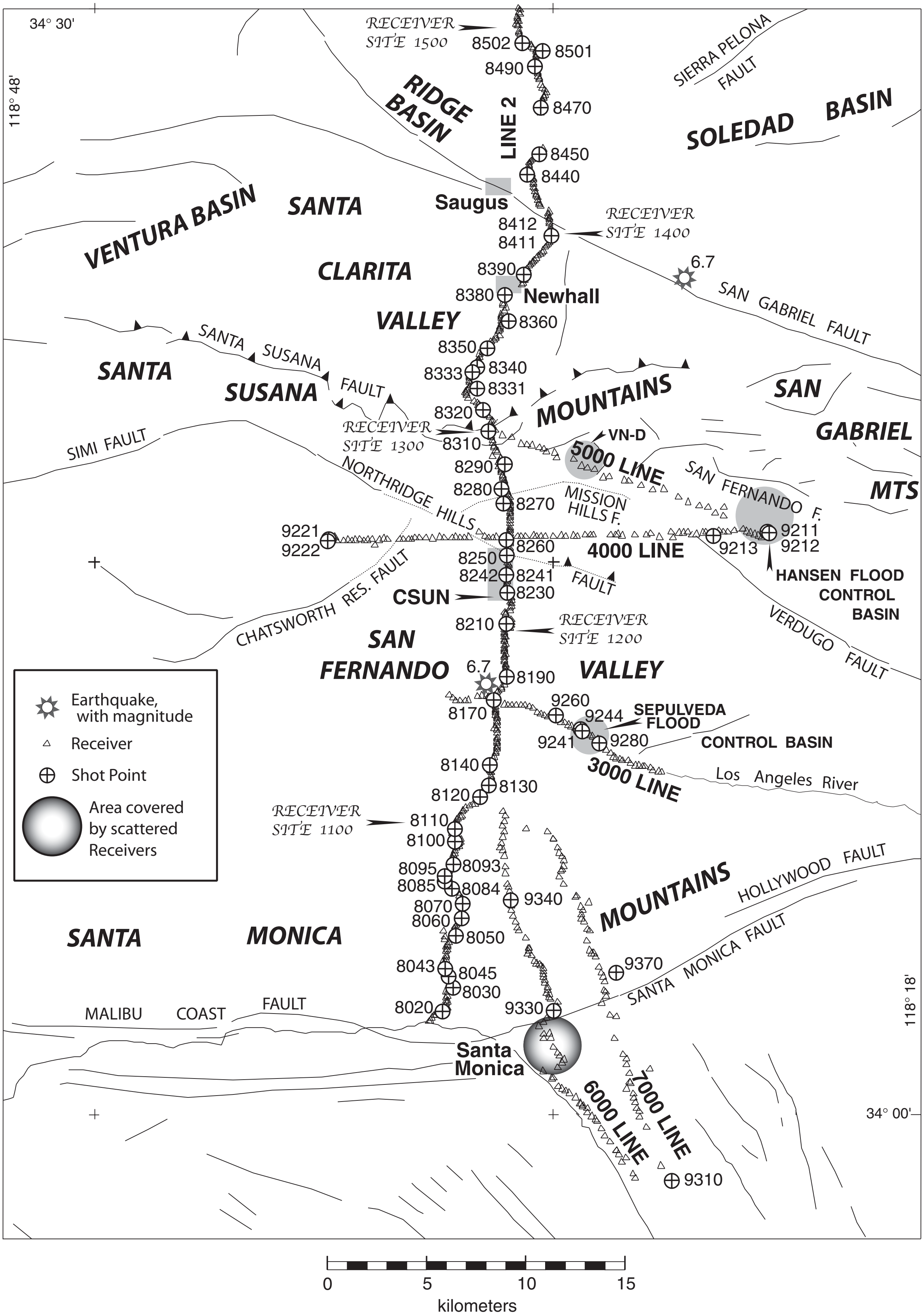

Figure 3. Fault map showing southern part of LARSE Line 2, auxiliary lines 3000-7000, and scatter deployment.

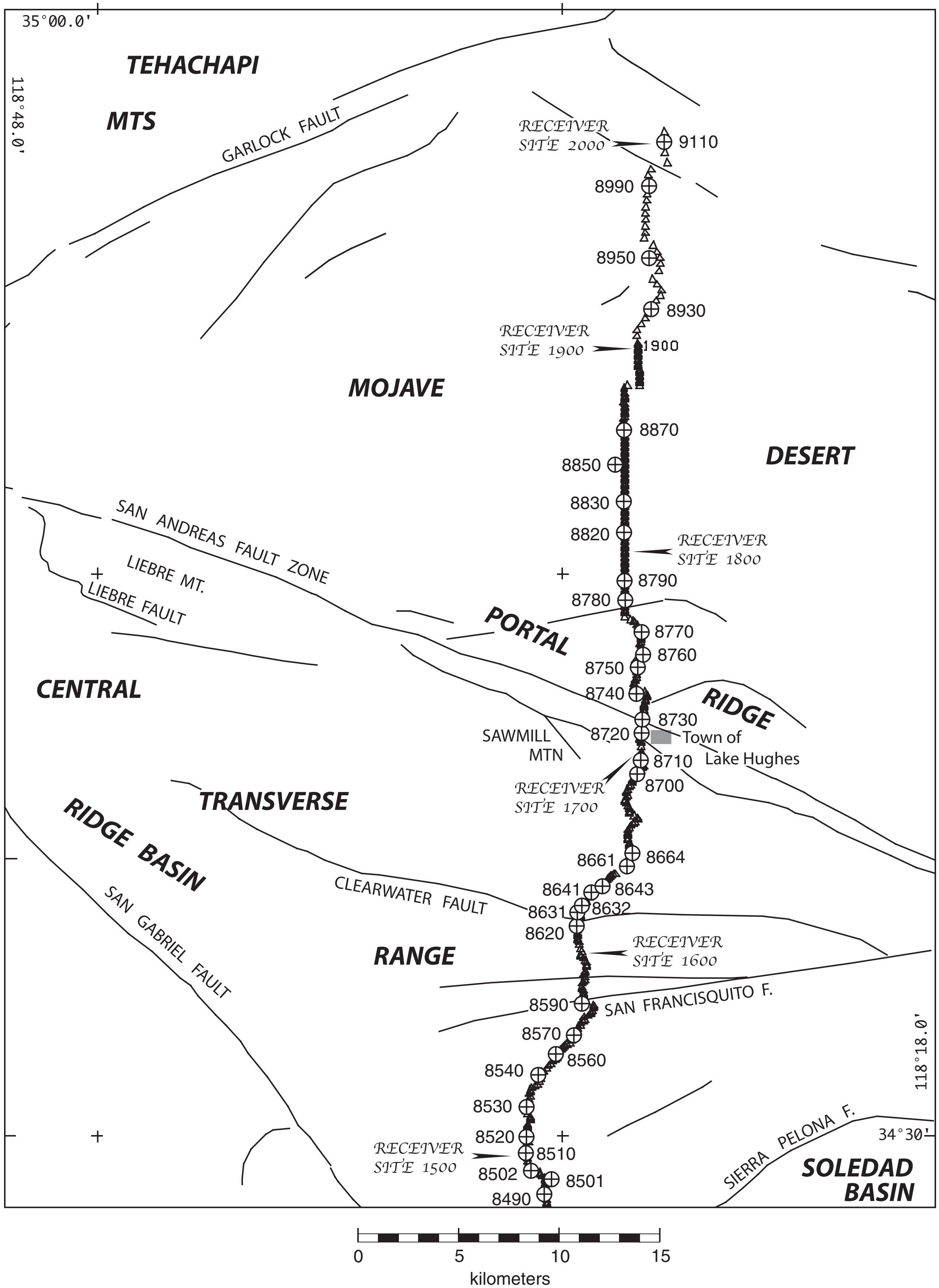

Figure 4. Fault map showing central part of LARSE Line 2.

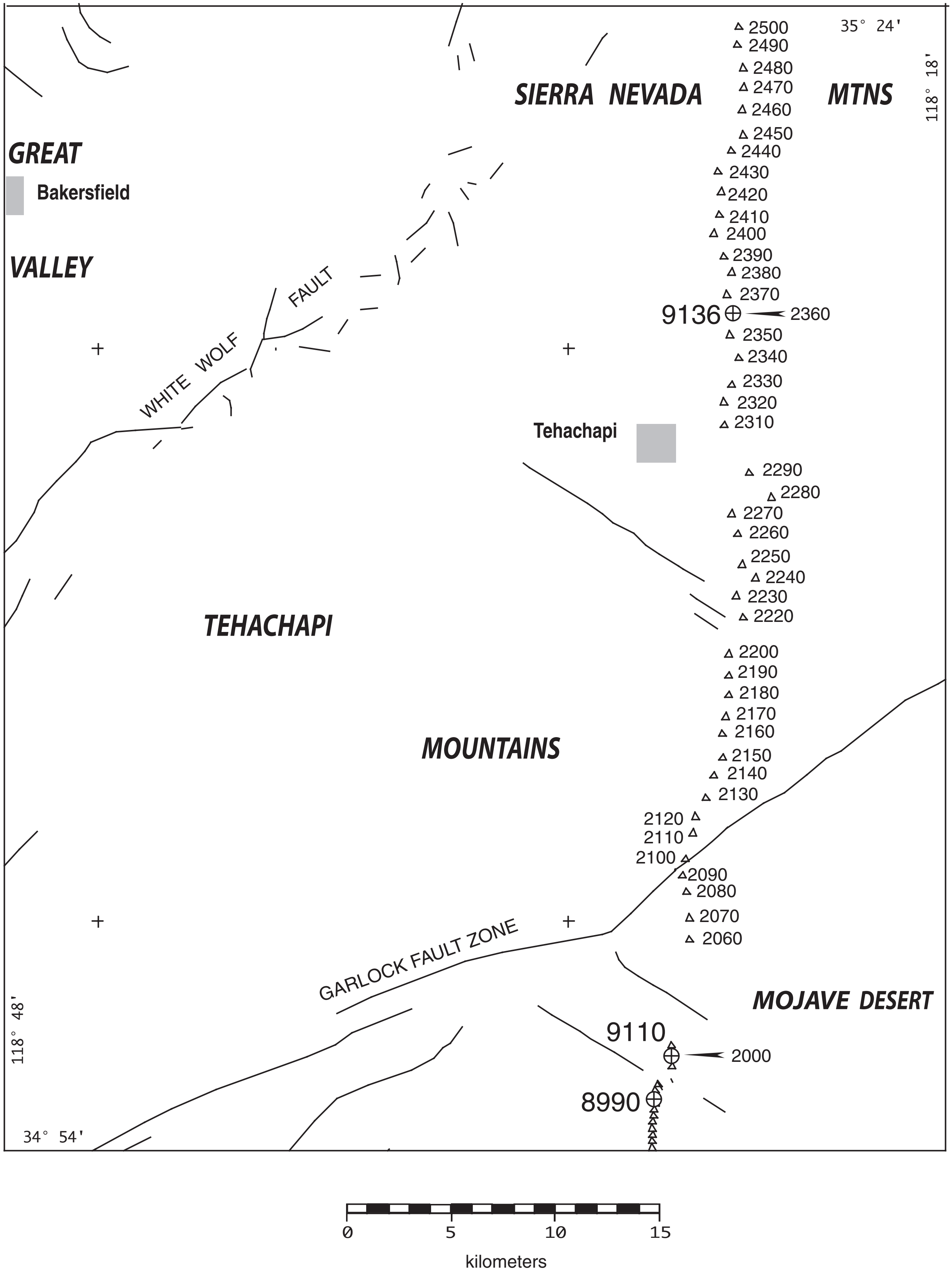

Figure 5. Fault map showing northern part of LARSE Line 2.

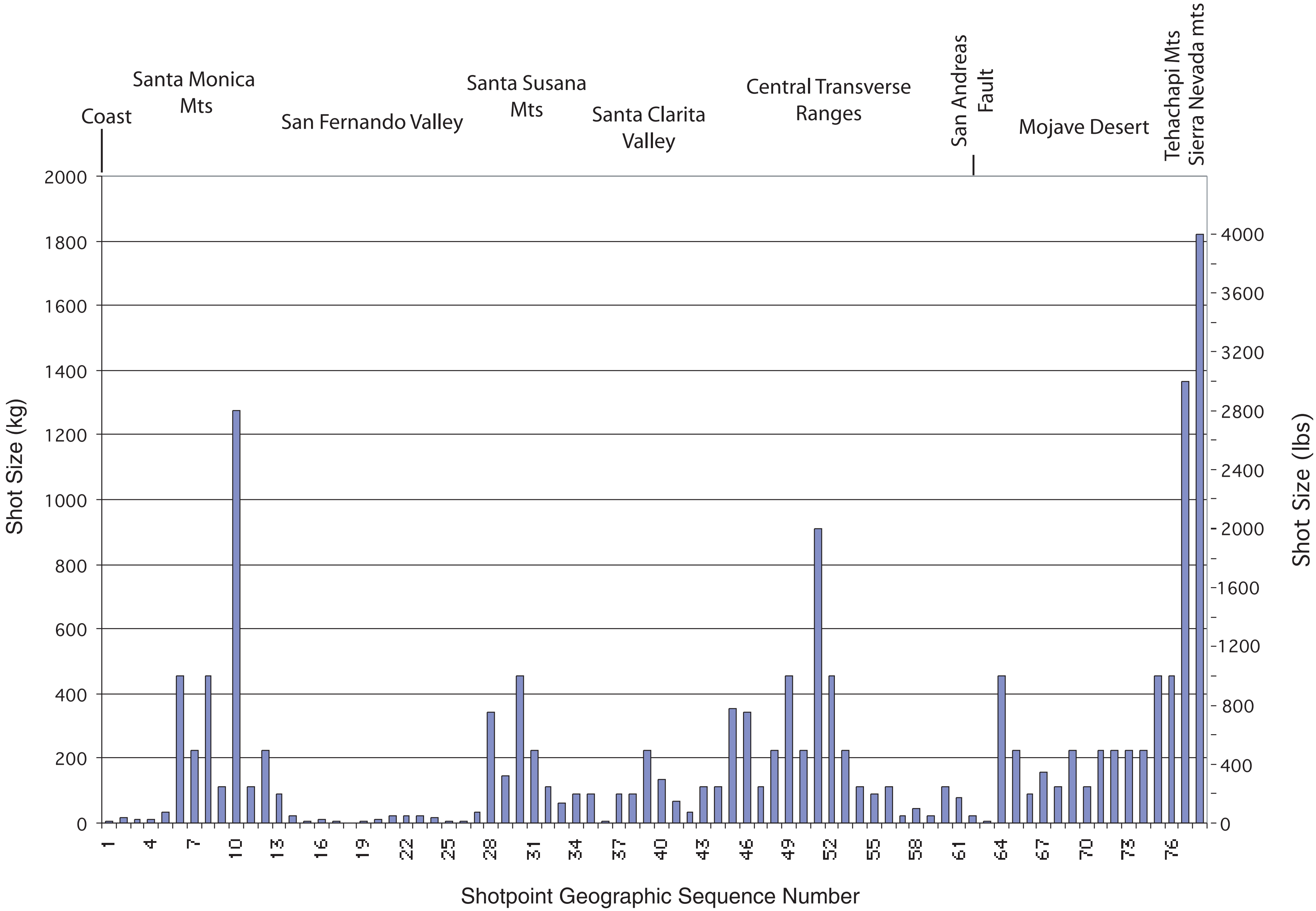

Figure 6. Shot size distribution along the main part of LARSE Line 2.

Figure 7. Shothole Diagram

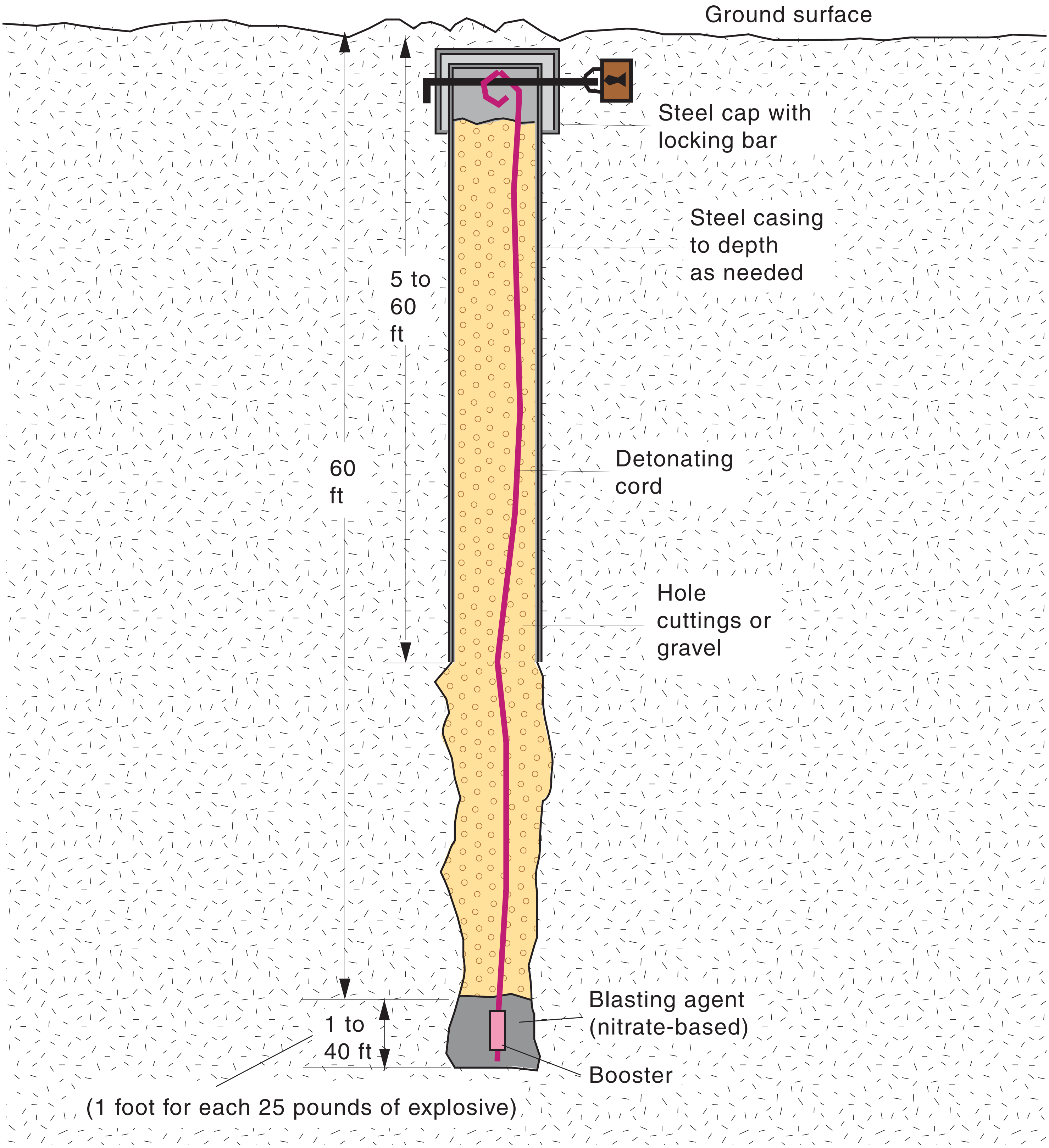

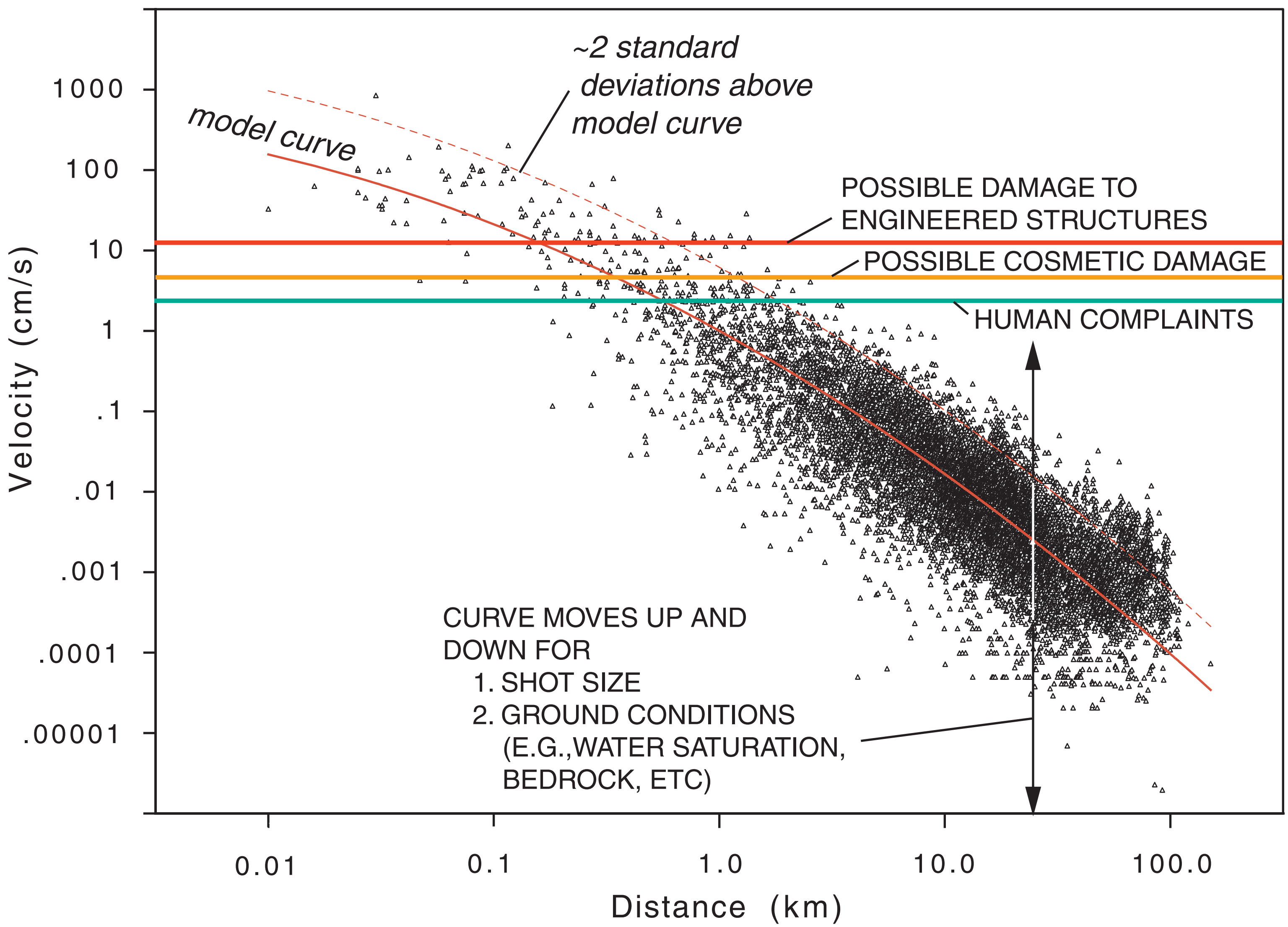

Figure 8. Seismic amplitudes (vertical ground velocity) versus distance, from LARSE I data and from calibration shots for LARSE II in San Fernando Valley

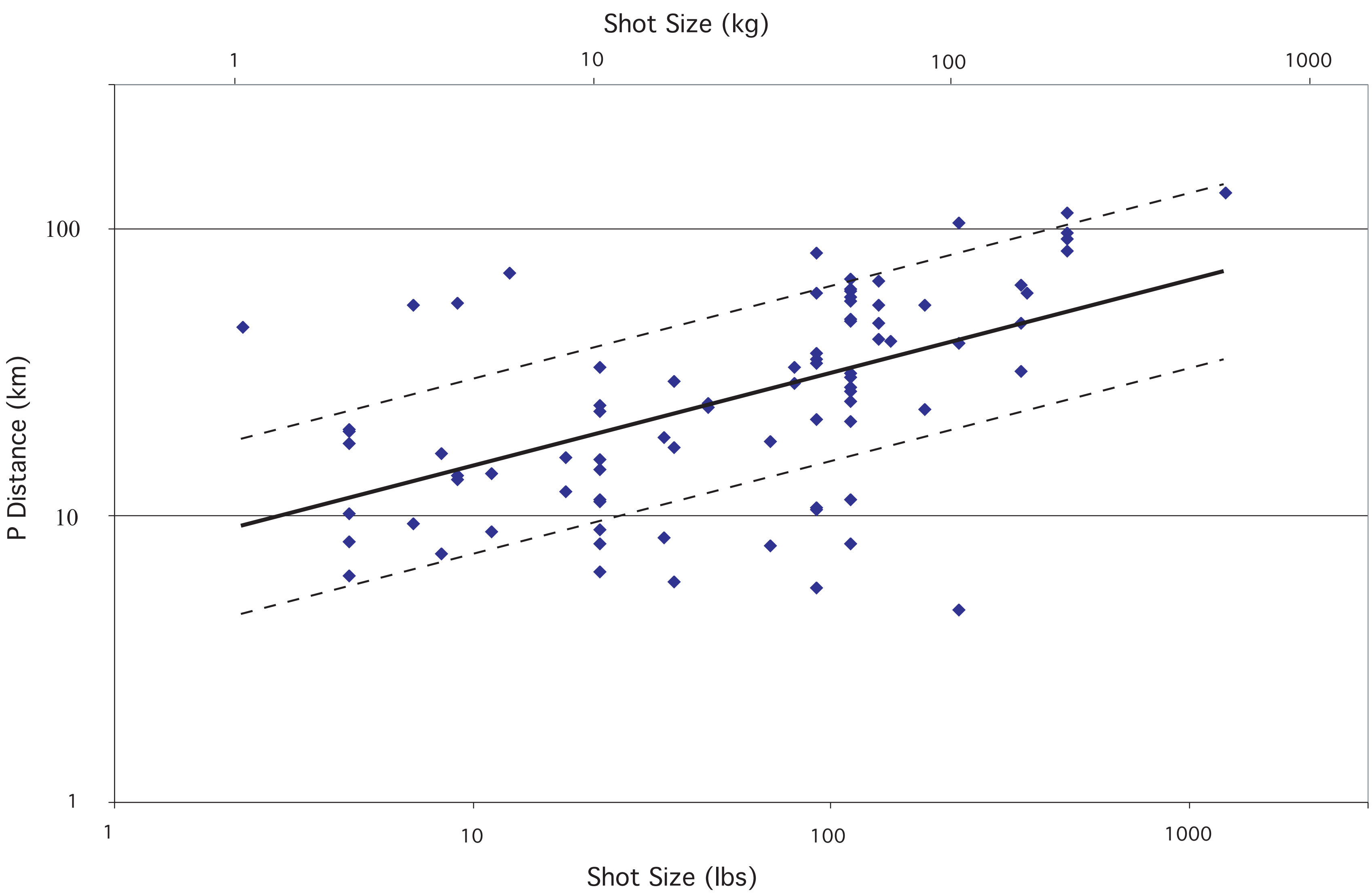

Figure 9. P-wave propagation distances versus shot size for all site conditions/geology (from Table 2b). The data are fit with a regression line (solid) and lines showing +1 and -1 standard deviations (dashed).

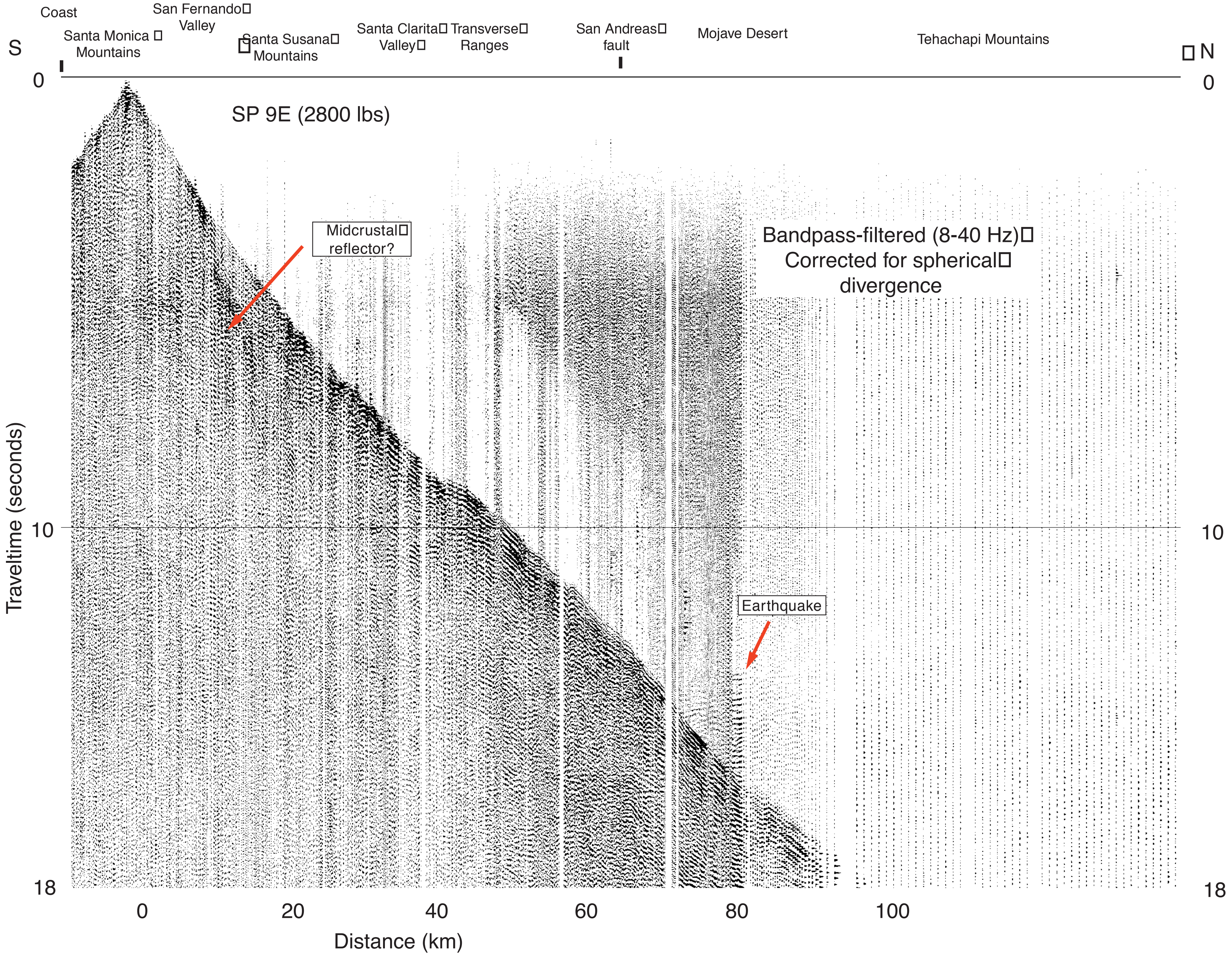

Figure 10. Data from Shotpoint 8095 (Sequence number 10)

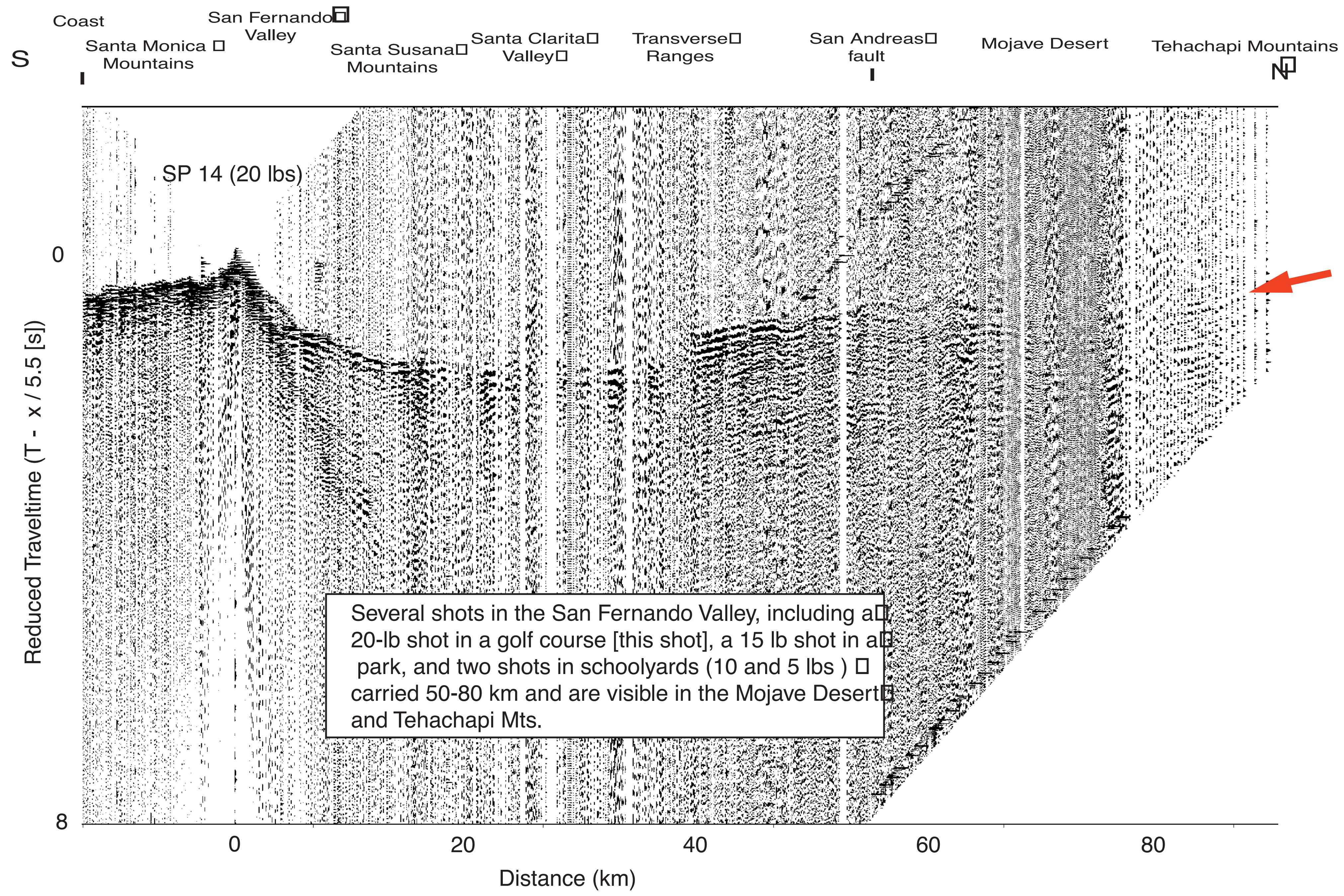

Figure 11. Data from Shotpoint 8140 (Sequence number 16)

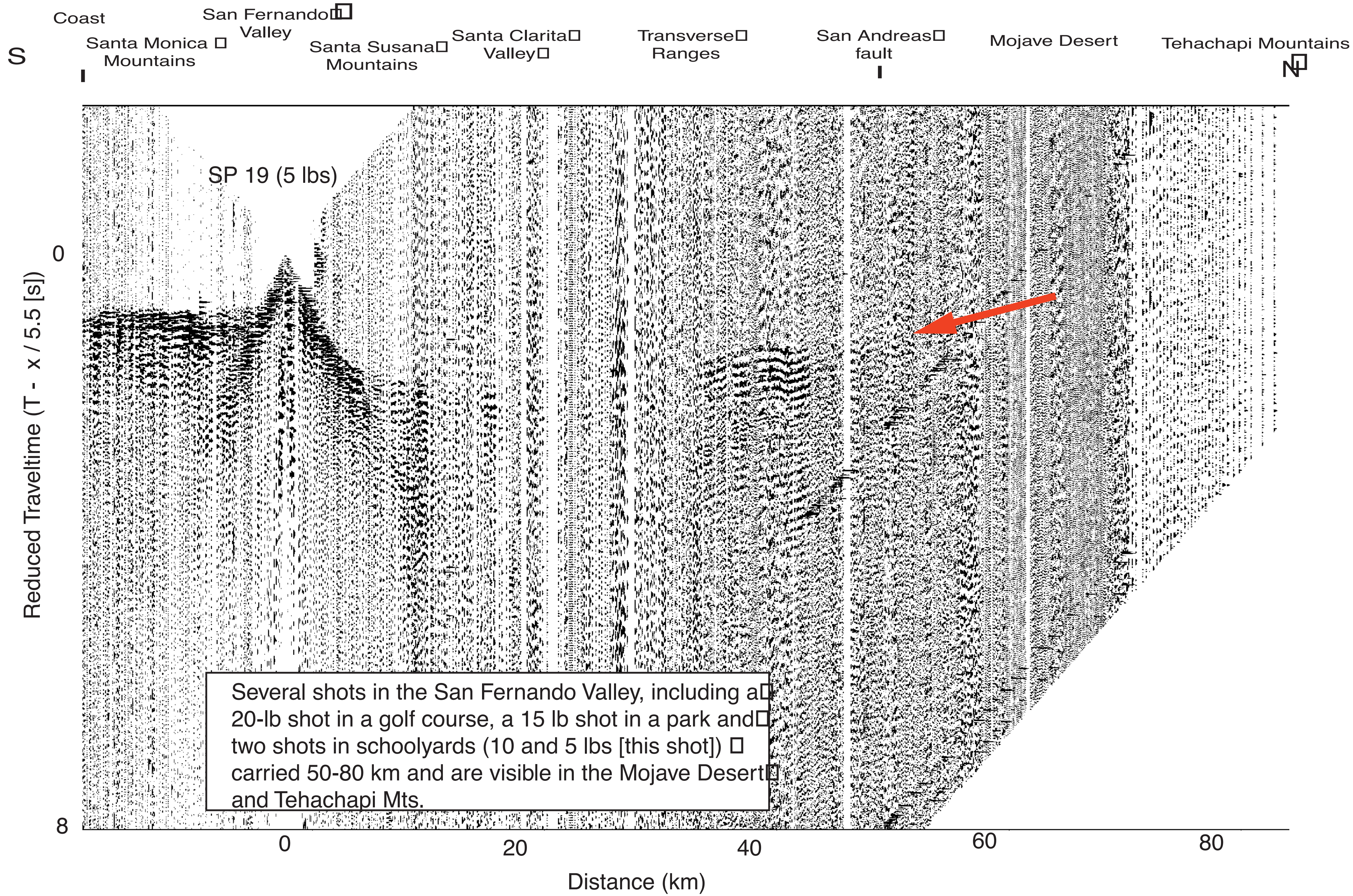

Figure 12. Data from Shotpoint 8190 (Sequence number 18)

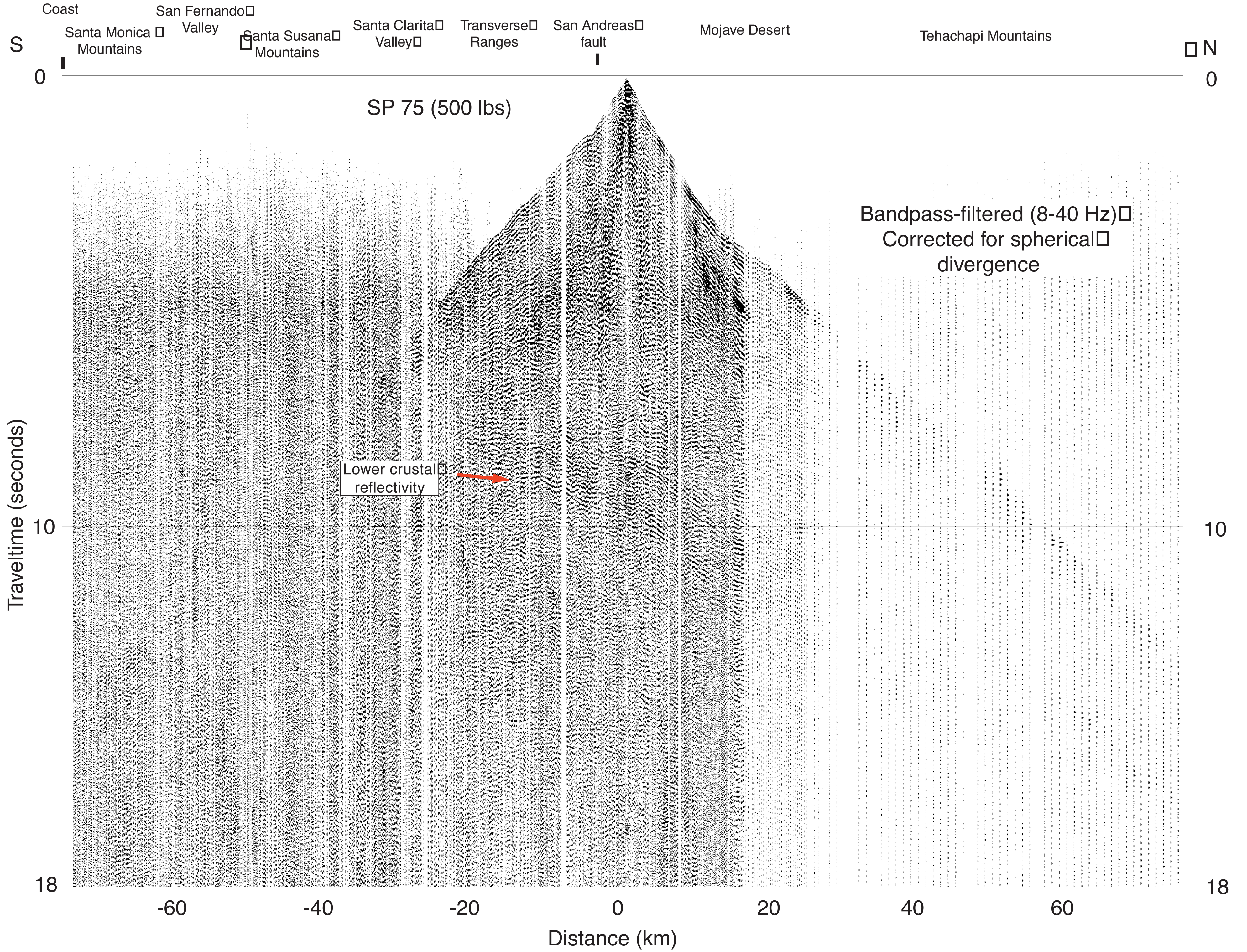

Figure 13. Data from Shotpoint 8740 (Sequence number 64)

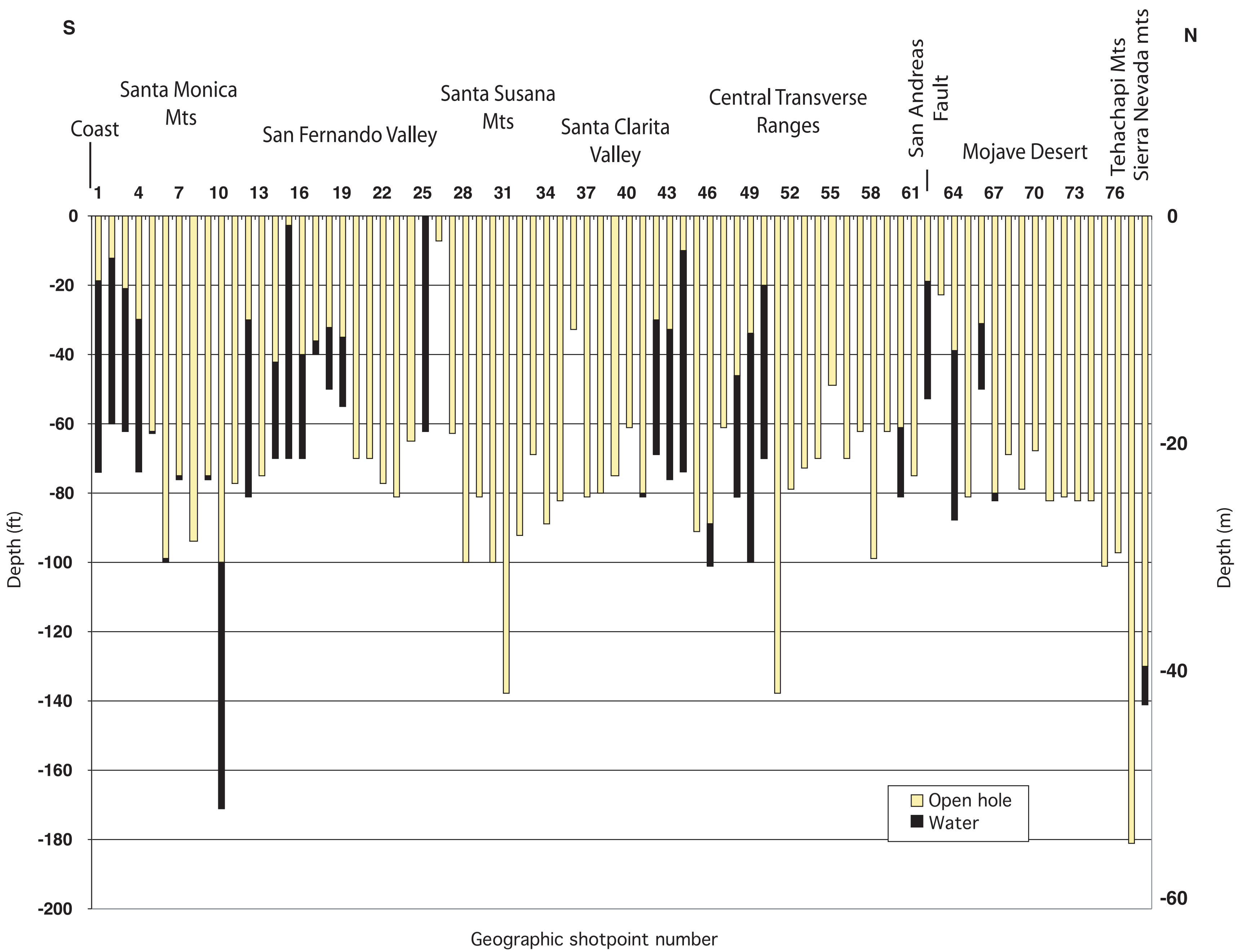

Figure 14. Profile of borehole depth and water-table depth along main part of LARSE Line 2.

Table 1. Seismographs - type, source, number, recording parameters.

Instrument type	Number	Data storage type	Disk size	A-D bit size	Timing type	Jug freq (hz)	System bandpass	Jug components	Sample rate (sps)
IRIS Refteks	246	disk	230 (112); 540 (84); 1Gb (44)	16-bit (92) 24-bit (148)	98 - int. GPS; 98 - ext. GPS; 45 - internal clock accuracy 1.0 ppm	4.5	4.5-200	3	250
Texans	540	RAM	32 Mb	24-bit	internal clock accuracy 0.1 ppm	4.5	4.5-200	1	250
PRS1's	176	RAM	1 Mb	12-bit gain-ranged	internal clock accuracy 0.1 ppm	2	~2-25	1	120
PRS4's	28	RAM	3-5 Mb					3	
SGR's	180	tape		16-bit (96db)	internal clock accuracy 0.1 ppm	8	8-200	1	500
German Teledyne PDAS-100 (34 x 6-ch)	204	disk	1 Gb	16 bit gain-ranged	internal clock accuracy 0.1 ppm	4.5	4.5-160	1	200
USGS Refteks	10	disk	4 Gb	24-bit	external GPS	2Hz/100 Hz	2-200	6 2-Hz velocity sensors and 3 Force-Balance Accelerometers	250
SCEC Refteks	18								
LLL Refteks	3								
Total	1405								

Table 1. Seismographs - type, source, number, recording parameters.

Instrument type	Power duration	No. Prog windows	Max window length	Deployment Constraints: Data Storage	Deployment Constraints: Clock Timing	Summary	Mid-stream Service
IRIS Refteks	a. 10 days b. 12 days	inf.	inf.	none none	45 have no GPS: need pulsing every 2 days	Refteks stay out; 45 pulsed every 2 days	QC batteries/ DAS status
Texans	5-6 days	999	variable	none	5 day max	batteries last ony 5 days; clock drift	bring in (field service possible?); reprogram; change batteries
PRS1's	10 days	130 (30 sec)	540 s	130 windows	5 day max	3-night window limit; clock drift	in field with field units (~3-4) download data; reprogram
PRS4's							
SGR's	5-6 days	99	99	daily tape change (23-25 min/tape)	5 day max	daily tape change; 3-night window limit	in field with laptops (~4-5) reprogram; if bring in, can recharge batteries
German Teledyne PDAS-100 (34 x 6-ch)	10 day	inf.	inf.	none	none	battery cycle program	in field
USGS Refteks	10 days	inf.	inf.	none	none		QC batteries/ DAS status
SCEC Refteks							
LLL Refteks							

Table 2a. Shot list

Geographic Shotpoint Sequence Number	Chronologic SP Sequence Number == SEGY Bytes 9-12 "Shot Gather Index Number" or "FFID"	Julian Day	UTC (HH:MM:SS.00)	Old Shotpoint Name	New Shotpoint Name == SEGY bytes 17-20 "SP"	Lat-WGS84	Long-WGS84	UTMx (NAD83)	UTMy (NAD83)	Elevation (ft above Mean Sea Level)	Elevation (m above Mean Sea Level)	Shot size (kg)	Shot size (lbs)
1	82	297	11:30:00.000	2A	8020	-118.56047	34.04698	355967	3768463	226	69	8	18
2	72	297	10:00:00.000	3E	8030	-118.55451	34.05772	356535	3769646	309	94	18	40
3	79	297	10:08:00.010	4E	8045	-118.55712	34.06279	356303	3770212	395	120	9	20
4	70	297	08:38:00.010	4C	8043	-118.55886	34.06632	356148	3770606	444	135	9	20
5	1	293	08:30:00.000	5H	8050	-118.55300	34.08115	356714	3772242	1467	447	36	80
6	12	293	10:00:00.000	6B	8060	-118.54980	34.08890	357022	3773097	1835	559	455	1000
7	19	293	11:30:00.000	7C	8070	-118.54954	34.09574	357058	3773855	1964	598	227	500
8	58	295	08:33:59.536	8D	8084	-118.55544	34.10216	356524	3774575	2043	623	455	1000
9	2	293	08:31:00.000	8E	8085	-118.55903	34.10533	356198	3774932	2003	610	114	250
10	13	293	10:01:00.000	9E	8095	-118.55900	34.10810	356206	3775239	2016	614	1273	2800
11	3	293	08:32:00.000	9C	8093	-118.55455	34.11358	356625	3775841	1828	557	114	250
12	14	293	10:02:00.000	10A	8100	-118.55243	34.12315	356837	3776899	1628	496	227	500
13	20	293	11:32:00.000	11A	8110	-118.55312	34.12921	356784	3777572	1680	512	91	200
14	64	297	08:31:00.000	12E	8120	-118.54007	34.14367	358011	3779157	964	294	23	50
15	73	297	10:01:00.000	13B	8130	-118.53530	34.14913	358460	3779756	922	281	8	18
16	83	297	11:31:00.000	14A	8140	-118.53481	34.15801	358520	3780740	849	259	9	20
17	74	297	10:02:00.000	17A	8170	-118.53272	34.18802	358763	3784065	725	221	7	15
18	84	297	11:32:00.000	19	8190	-118.52556	34.19816	359440	3785180	733	223	2	5
19	93	298	08:30:00.000	21	8210	-118.52587	34.22236	359451	3787864	777	237	5	10
20	68	297	08:36:00.000	23A	8230	-118.52501	34.23614	359553	3789391	849	259	11	25
21	77	297	10:06:00.000	24 (1)	8241	-118.52542	34.24451	359530	3790320	898	274	23	50
22	88	297	11:36:00.000	24 (2)	8242	-118.52559	34.24458	359514	3790328	899	274	23	50
23	76	297	10:05:00.000	25	8250	-118.52537	34.25293	359548	3791253	968	295	23	50
24	67	297	08:35:00.000	26A	8260	-118.52545	34.26001	359553	3792039	1000	305	18	40
25	87	297	11:35:26.780	27A	8270	-118.52716	34.27682	359423	3793905	1118	341	7	15
26	85	297	11:33:00.000	28	8280	-118.52828	34.28352	359331	3794650	1178	359	5	10
27	65	297	08:33:00.000	29A	8290	-118.52663	34.29431	359501	3795844	1339	408	34	75
28	4	293	08:33:00.000	31A	8310	-118.53577	34.30932	358685	3797521	2593	790	341	750
29	15	293	10:03:00.000	32A	8320	-118.53841	34.31914	358458	3798614	2578	786	148	325
30	21	293	11:33:00.000	33A	8331	-118.54200	34.32845	358144	3799651	2554	778	455	1000

Table 2a. Shot list

Geographic Shotpoint Sequence Number	Chronologic SP Sequence Number == SEGY Bytes 9-12 "Shot Gather Index Number" or "FFID"	Julian Day	UTC (HH:MM:SS.00)	Old Shotpoint Name	New Shotpoint Name == SEGY bytes 17-20 "SP"	Lat-WGS84	Long-WGS84	UTMx (NAD83)	UTMy (NAD83)	Elevation (ft above Mean Sea Level)	Elevation (m above Mean Sea Level)	Shot size (kg)	Shot size (lbs)
31	29	294	08:33:00.000	33C	8333	-118.54446	34.33581	357930	3800471	2179	664	227	500
32	48	294	11:33:00.000	34A	8340	-118.54144	34.33823	358212	3800735	1803	550	114	250
33	57	295	08:33:00.000	35B	8350	-118.53598	34.34664	358728	3801660	1603	489	59	130
34	35	294	08:39:00.000	36D	8360	-118.52438	34.35874	359815	3802986	1491	455	91	200
35	44	294	10:09:00.000	38A	8380	-118.52656	34.37048	359634	3804291	1542	470	91	200
36	53	294	11:39:00.000	39A	8390	-118.51635	34.38016	360589	3805351	1316	401	5	10
37	18	293	10:10:00.000	41C(1-east)	8411	-118.50124	34.39784	362008	3807291	1665	508	91	200
38	25	293	11:40:00.000	41C(2)	8412	-118.50143	34.39781	361990	3807287	1662	507	91	200
39	11	293	08:40:00.000	44C	8440	-118.51421	34.42535	360861	3810359	1409	430	227	500
40	54	294	11:40:00.000	45B	8450	-118.50794	34.43455	361452	3811371	1604	489	136	300
41	45	294	10:10:00.000	47F	8470	-118.50685	34.45523	361587	3813663	1395	425	68	150
42	36	294	08:40:00.000	49B	8490	-118.50973	34.47410	361353	3815759	1450	442	36	80
43	49	294	11:34:00.000	50B1	8501	-118.50596	34.48101	361711	3816521	1519	463	114	250
44	39	294	10:04:00.000	50B2	8502	-118.51678	34.48458	360723	3816931	1570	479	114	250
45	30	294	08:34:00.000	51B	8510	-118.51962	34.49244	360475	3817807	1962	598	352	775
46	50	294	11:35:00.000	52B	8520	-118.51915	34.49961	360531	3818601	1876	572	341	750
47	40	294	10:05:00.000	53B	8530	-118.51939	34.51317	360531	3820106	1976	602	114	250
48	22	293	11:35:00.000	54B	8540	-118.51319	34.52749	361124	3821685	2005	611	227	500
49	16	293	10:05:00.000	56A	8560	-118.50337	34.53634	362040	3822653	2112	644	455	1000
50	6	293	08:35:00.000	57A	8570	-118.49386	34.54494	362927	3823594	2150	655	227	500
51	31	294	08:35:00.000	59B	8590	-118.48955	34.55900	363345	3825147	1658	505	909	2000
52	56	295	08:32:00.000	62	8620	-118.49236	34.59331	363144	3828956	2846	867	455	1000
53	55	295	08:31:00.000	63A	8631	-118.49185	34.59964	363201	3829658	3134	955	227	500
54	59	295	08:36:00.000	63B	8632	-118.48947	34.60275	363424	3829999	3296	1005	114	250
55	23	293	11:36:00.000	64A	8641	-118.48452	34.60843	363887	3830622	3462	1055	91	200
56	17	293	10:06:00.000	64C	8643	-118.47867	34.61118	364428	3830920	3627	1106	114	250
57	7	293	08:36:00.000	65A	8650	-118.47038	34.61698	365198	3831552	3833	1168	23	50
58	32	294	08:36:00.000	66A	8661	-118.46532	34.61998	365667	3831878	3755	1144	45	100
59	41	294	10:06:00.000	66D	8664	-118.46244	34.62581	365940	3832520	3808	1161	23	50
60	62	295	10:00:00.000	70C	8700	-118.45985	34.66074	366234	3836391	2852	869	114	250

Table 2a. Shot list

Geographic Shotpoint Sequence Number	Chronologic SP Sequence Number == SEGY Bytes 9-12 "Shot Gather Index Number" or "FFID"	Julian Day	UTC (HH:MM:SS.00)	Old Shotpoint Name	New Shotpoint Name == SEGY bytes 17-20 "SP"	Lat-WGS84	Long-WGS84	UTMx (NAD83)	UTMy (NAD83)	Elevation (ft above Mean Sea Level)	Elevation (m above Mean Sea Level)	Shot size (kg)	Shot size (lbs)
61	61	295	08:40:00.000	71A	8710	-118.45786	34.66724	366426	3837109	3324	1013	80	175
62	8	293	08:37:00.000	72A	8720	-118.45747	34.67920	366481	3838435	3029	923	23	50
63	24	293	11:37:00.000	73A	8730	-118.45713	34.68530	366522	3839111	3223	982	5	10
64	60	295	08:37:00.000	74A	8740	-118.46050	34.69654	366232	3840362	3595	1096	455	1000
65	51	294	11:37:00.000	75A	8750	-118.45971	34.70829	366323	3841664	3457	1054	227	500
66	42	294	10:07:00.000	76A	8760	-118.45659	34.71417	366618	3842312	3003	915	91	200
67	33	294	08:37:00.000	77A	8770	-118.45744	34.72401	366556	3843404	2778	847	159	350
68	28	294	08:32:00.000	78	8780	-118.46644	34.73835	365755	3845007	2698	822	114	250
69	38	294	10:02:00.000	79	8790	-118.46660	34.74652	365754	3845913	2666	813	227	500
70	47	294	11:32:00.000	82	8820	-118.46714	34.76808	365739	3848305	2600	792	114	250
71	27	294	08:31:00.000	83A	8830	-118.46687	34.78204	365787	3849853	2554	778	227	500
72	37	294	10:01:00.000	85C	8850	-118.47170	34.79846	365371	3851680	2503	763	227	500
73	46	294	11:31:00.000	87	8870	-118.46714	34.81357	365813	3853350	2477	755	227	500
74	52	294	11:38:00.010	93	8930	-118.45226	34.86724	367260	3859282	2673	815	227	500
75	43	294	10:08:00.010	95	8950	-118.45371	34.88991	367164	3861799	3170	966	455	1000
76	34	294	08:38:00.009	99	8990	-118.45366	34.92157	367220	3865310	3400	1036	455	1000
77	26	294	08:30:00.000	101	9110	-118.44512	34.94142	368032	3867500	3760	1146	1364	3000
78	9	293	08:38:00.010	136	9136	-118.41124	35.26513	371634	3903358	3440	1049	1818	4000
79	81	297	10:10:00.000	301	9310	-118.43540	33.97048	367393	3759811	4	1	182	400
80	90	297	11:38:00.009	303	9330	-118.50003	34.04785	361547	3768476	280	85	13	28
81	63	297	08:30:00.000	304	9340	-118.52307	34.09754	359503	3774018	1443	440	455	1000
82	5	293	08:34:00.000	305	9350	-118.74382	34.61580	340125	3831820	1905	581	1818	4000
83	92	297	11:40:00.000	307	9370	-118.46585	34.06485	364729	3770316	447	136	23	50
84	10	293	08:39:00.000	306	9360	-118.76061	34.81881	338979	3854363	3345	1020	1705	3750
85	69	297	08:37:01.992	208	9280	-118.47471	34.16904	364078	3781882	680	207	136	300
86	78	297	10:07:00.000	204C4	9244	-118.48437	34.17447	363197	3782497	695	212	295	650
87	89	297	11:37:00.000	204C1	9241	-118.48403	34.17406	363228	3782451	698	213	182	400
88	66	297	08:34:00.000	206	9260	-118.49816	34.18138	361937	3783282	700	213	136	300
89	80	297	10:09:00.000	201 (1-north)	9211	-118.38348	34.26461	372632	3792362	990	302	227	500
90	91	297	11:39:00.000	201 (2--south)	9212	-118.38365	34.26435	372616	3792333	990	302	455	1000

Table 2a. Shot list

Geographic Shotpoint Sequence Number	Chronologic SP Sequence Number == SEGY Bytes 9-12 "Shot Gather Index Number" or "FFID"	Julian Day	UTC (HH:MM:SS.00)	Old Shotpoint Name	New Shotpoint Name == SEGY bytes 17-20 "SP"	Lat-WGS84	Long-WGS84	UTMx (NAD83)	UTMy (NAD83)	Elevation (ft above Mean Sea Level)	Elevation (m above Mean Sea Level)	Shot size (kg)	Shot size (lbs)
91	71	297	08:39:00.000	201C	9213	-118.41303	34.26225	369907	3792138	1015	309	36	80
92	75	297	10:04:00.000	202B1(north)	9221	-118.62223	34.26090	350643	3792275	1061	323	136	300
93	86	297	11:34:00.000	202B2(south)	9222	-118.62221	34.26075	350644	3792259	1068	326	136	300

Table 2B--Additional Shotpoint Information

Geo-graphic shot-point sequence no.	Shotpoint name	Hole depth (m)	Hole depth (ft)	Depth to to water before loading (m)	Depth to to water before loading (ft)	Water column in hole before loading (m)	Water column in hole before loading (ft)	Charge Size (kg)	Charge size (lbs)	Depth to top of explosive (m)	Depth to top of explosive (ft)	Surface geology	Geol. site label	South: max. dist. clear P arrival	North: max. dist. clear P arrival	South: max dist. clear energy	North: max dist clear energy
1	8020	22.6	74	5.8	19	16.8	55	8.2	18	21.9	72	T sed	S	-	16.3	-	69.8
2	8030	18.3	60	3.7	12	14.6	48	18.1	40	18.3	60	T sed	S	-	15.8	-	60.9
3	8045	18.9	62	6.4	21	12.5	41	9.1	20	18.3	60	T sed	S	-	13.4	-	13.4
4	8043	22.6	74	9.1	30	13.4	44	9.1	20	22.3	73	T sed	S	-	13.8	-	16.9
5	8050	19.2	63	18.9	62	0.3	1	36.3	80	19.2	63	T sed	S	-	5.9	-	7.2
6	8060	30.5	100	30.2	99	0.3	1	453.6	1000	18.9	62	T sed	S	-	112.7	-	-
7	8070	23.2	76	22.9	75	0.3	1	226.8	500	19.2	63	T sed	S	-	103.8	-	-
8	8084	28.7	94	28.7	94	0.0	0	453.6	1000	19.2	63	T sed	S	-	96.1	-	-
9	8085	23.2	76	22.9	75	0.3	1	113.4	250	21.9	72	T sed	S	-	55.5	-	68.3
10	8095	52.1	171	30.5	100	21.6	71	1270.1	2800	33.5	110	T sed	S	-	132.8	-	-
11	8093	23.5	77	23.5	77	0.0	0	113.4	250	20.4	67	T sed	S	-	60.2	-	82.3
12	8100	24.7	81	9.1	30	15.5	51	226.8	500	21.6	71	T sed	S	-	4.7	-	10.0
13	8110	22.9	75	22.9	75	0.0	0	90.7	200	20.4	67	T sed	S	-	59.8	-	67.8
14	8120	21.3	70	12.8	42	8.5	28	22.7	50	20.7	68	T sed	S	-	8.0	-	9.5
15	8130	21.3	70	0.9	3	20.4	67	8.2	18	21.0	69	T sed	S	-	7.3	-	9.2
16	8140	21.3	70	12.2	40	9.1	30	9.1	20	21.0	69	T sed	S	-	54.7	-	96.8
17	8170	12.2	40	11.0	36	1.2	4	6.8	15	12.2	40	wet Q alluv	A	-	54.0	-	98.5
18	8190	15.2	50	9.8	32	5.5	18	2.3	5	15.2	50	wet Q alluv	A	-	44.9	-	52.8
19	8210	16.8	55	10.7	35	6.1	20	4.5	10	16.8	55	wet Q alluv	A	19.5	10.2	-	17.0
20	8230	21.3	70	21.3	70	0.0	0	11.3	25	20.7	68	dry Q alluv	D	14.0	8.7	15.7	13.9
21	8241	21.3	70	21.3	70	0.0	0	22.7	50	20.7	68	dry Q alluv	D	-	11.3	-	47.9
22	8242	23.5	77	23.5	77	0.0	0	22.7	50	22.9	75	dry Q alluv	D	-	32.9	-	47.7
23	8250	24.7	81	24.7	81	0.0	0	22.7	50	24.1	79	dry Q alluv	D	-	6.4	-	8.2
24	8260	19.8	65	19.8	65	0.0	0	18.1	40	19.8	65	dry Q alluv	D	-	12.1	-	35.5
25	8270	18.9	62	0.0	0	18.9	62	6.8	15	18.9	62	wet Q alluv	A	-	9.4	-	42.2
26	8280	2.1	7	2.1	7	0.0	0	4.5	10	2.1	7	wet Q alluv	A	3.9	-	-	-
27	8290	19.2	63	19.2	63	0.0	0	34.0	75	18.3	60	dry QT alluv	D	18.8	8.3	-	32.7
28	8310	30.5	100	30.5	100	0.0	0	340.2	750	21.3	70	T sed	S	-	31.6	-	-
29	8320	24.7	81	24.7	81	0.0	0	147.4	325	21.0	69	T sed (landslide)	S	-	40.5	-	81.1
30	8331	30.5	100	30.5	100	0.0	0	453.6	1000	17.7	58	T sed	S	-	83.2	-	-
31	8333	42.1	138	42.1	138	0.0	0	226.8	500	38.7	127	T sed / methane	S				
32	8340	28.0	92	28.0	92	0.0	0	113.4	250	23.8	78	T sed / methane	S	30.4	66.0	-	-

Table 2B--Additional Shotpoint Information

Geo-graphic shot-point sequence no.	Shotpoint name	Hole depth (m)	Hole depth (ft)	Depth to to water before loading (m)	Depth to to water before loading (ft)	Water column in hole before loading (m)	Water column in hole before loading (ft)	Charge Size (kg)	Charge size (lbs)	Depth to top of explosive (m)	Depth to top of explosive (ft)	Surface geology	Geol. site label	South: max. dist. clear P arrival	North: max. dist. clear P arrival	South: max dist. clear energy	North: max dist clear energy
33	8350	21.0	69	21.0	69	0.0	0	59.0	130	18.3	60	T sed	S				
34	8360	27.1	89	27.1	89	0.0	0	113.4	250	24.4	80	dry QTalluv	D	-	81.6	-	-
35	8380	25.0	82	25.0	82	0.0	0	90.7	200	23.5	77	dry QTalluv	D	35.0	33.9	-	41.0
36	8390	10.1	33	10.1	33	0.0	0	4.5	10	8.5	28	dry QTalluv	D	8.1	6.2	8.1	23.6
37	8411	24.7	81	24.7	81	0.0	0	90.7	200	22.6	74	dry QTalluv	D	-	36.9	-	58.4
38	8412	24.4	80	24.4	80	0.0	0	90.7	200	21.9	72	dry QTalluv	D	5.6	21.6	37.3	29.7
39	8440	22.9	75	22.9	75	0.0	0	226.8	500	16.8	55	dry QTalluv	D	-	-	-	-
40	8450	18.6	61	18.6	61	0.0	0	136.1	300	15.2	50	dry QTalluv	D	-	65.2	-	-
41	8470	24.7	81	24.4	80	0.3	1	68.0	150	24.1	79	wet QTalluv	A	7.8	18.2	10.9	25.8
42	8490	21.0	69	9.1	30	11.9	39	36.3	80	19.8	65	T sed	S	17.2	29.5	-	51.1
43	8501	23.2	76	10.1	33	13.1	43	113.4	250	21.6	71	T sed	S	-	60.9	-	-
44	8502	22.6	74	3.0	10	19.5	64	113.4	250	19.2	63	T sed	S	-	-	-	-
45	8510	27.7	91	27.7	91	0.0	0	351.5	775	17.7	58	T sed	S	-	59.0	-	-
46	8520	30.8	101	27.1	89	3.7	12	340.2	750	21.3	70	T sed	S	46.3	63.2	-	-
47	8530	18.6	61	18.6	61	0.0	0	113.4	250	15.5	51	T sed	S	48.3	57.5	-	67.6
48	8540	24.7	81	14.0	46	10.7	35	226.8	500	18.6	61	Pelona Schist	R	-	-	-	-
49	8560	30.5	100	10.4	34	20.1	66	453.6	1000	15.2	50	Pelona Schist	R	-	-	-	-
50	8570	21.3	70	6.1	20	15.2	50	226.8	500	20.1	66	Pelona Schist	R	-	-	-	-
51	8590	42.1	138	42.1	138	0.0	0	907.2	2000	21.9	72	Pelona Schist	R	-	-	-	-
52	8620	24.1	79	24.1	79	0.0	0	453.6	1000	16.5	54	PC ign-meta rock	R	-	-	-	-
53	8631	22.3	73	22.3	73	0.0	0	226.8	500	16.2	53	PC ign-meta rock	R	57.6	-	-	-
54	8632	21.3	70	21.3	70	0.0	0	113.4	250	19.8	65	PC ign-meta rock	R	21.1	47.3	24.4	-
55	8641	14.9	49	14.9	49	0.0	0	90.7	200	13.7	45	PC ign-meta rock	R	22.2	-	25.1	-
56	8643	21.3	70	21.3	70	0.0	0	113.4	250	17.7	58	PC ign-meta rock	R	59.4	-	-	-
57	8650	18.9	62	18.9	62	0.0	0	22.7	50	17.7	58	PC ign-meta rock	R	22.9	24.0	22.9	26.0
58	8661	30.2	99	30.2	99	0.0	0	45.4	100	18.0	59	PC ign-meta rock	R	24.4	23.6	62.5	55.0

Table 2B--Additional Shotpoint Information

Geo-graphic shot-point sequence no.	Shotpoint name	Hole depth (m)	Hole depth (ft)	Depth to to water before loading (m)	Depth to to water before loading (ft)	Water column in hole before loading (m)	Water column in hole before loading (ft)	Charge Size (kg)	Charge size (lbs)	Depth to top of explosive (m)	Depth to top of explosive (ft)	Surface geology	Geol. site label	South: max. dist. clear P arrival	North: max. dist. clear P arrival	South: max dist. clear energy	North: max dist clear energy
59	8664	18.9	62	18.9	62	0.0	0	22.7	50	17.4	57	PC ign-meta rock	R	15.7	14.4	19.6	25.1
60	8700	24.7	81	18.6	61	6.1	20	113.4	250	21.6	71	PC ign-meta rock	R	11.3	8.0	13.4	10.4
61	8710	22.9	75	22.9	75	0.0	0	79.4	175	21.0	69	PC ign-meta rock	R	28.6	32.9	29.8	40.0
62	8720	16.2	53	5.8	19	10.4	34	22.7	50	14.9	49	PC ign-meta rock	R	31.0	-	69.0	-
63	8730	7.0	23	7.0	23	0.0	0	4.5	10	6.4	21	Mz ign	R	19.8	17.7	22.4	18.5
64	8740	26.8	88	11.9	39	14.9	49	453.6	1000	18.9	62	Mz ign	R	-	-	-	-
65	8750	24.7	81	24.7	81	0.0	0	226.8	500	19.2	63	Mz ign	R	25.4	-	67.8	-
66	8760	15.2	50	9.4	31	5.8	19	90.7	200	13.7	45	Mz ign	R	10.4	10.6	16.7	22.8
67	8770	25.0	82	24.4	80	0.6	2	158.8	350	24.4	80	wet Q alluv	A	27.2	-	-	-
68	8780	21.0	69	21.0	69	0.0	0	113.4	250	19.2	63	dry Q alluv	D	27.7	25.0	28.3	56.5
69	8790	24.1	79	24.1	79	0.0	0	226.8	500	19.5	64	dry Q alluv	D	29.0	-	74.0	-
70	8820	20.7	68	20.7	68	0.0	0	113.4	250	18.6	61	dry Q alluv	D	26.8	31.0	32.6	-
71	8830	25.0	82	25.0	82	0.0	0	226.8	500	19.8	65	dry Q alluv	D	32.0	-	80.0	-
72	8850	24.7	81	24.7	81	0.0	0	226.8	500	21.3	70	dry Q alluv	D	35.0	-	80.0	-
73	8870	25.0	82	25.0	82	0.0	0	226.8	500	19.5	64	dry Q alluv	D	36.7	-	44.8	-
74	8930	25.0	82	25.0	82	0.0	0	226.8	500	19.5	64	dry Q alluv	D	38.4	-	42.1	-
75	8950	30.8	101	30.8	101	0.0	0	453.6	1000	21.3	70	dry Q alluv	D	43.9	-	45.2	-
76	8990	29.6	97	29.6	97	0.0	0	453.6	1000	22.3	73	dry Q alluv	D	48.8	-	94.0	-
77	9110	55.2	181	55.2	181	0.0	0	1360.8	3000	26.8	88	dry Q alluv	D	49.5	-	50.3	-
78	9136	43.0/ 43.0	141/ 141	39.6/ 39.6	130/ 130	3.4	11	1814.4	4000	22.6/ 22.6	74/ 74	Mz ign	R	101.1	-	-	-
79	9310	17.4	57	1.5	5	15.8	52	181.4	400	16.2	53	wet Q alluv	A	-	23.3	-	26.6
80	9330	31.1	102	21.3	70	9.8	32	12.7	28	30.5	100	wet Q alluv	A	-	69.6	-	110.0
81	9340	30.5	100	30.5	100	0.0	0	453.6	1000	22.9	75	Mz ign	R	-	91.8	-	-
82	9350	43.0/ 43.0	141/ 141	12.2/ 4.1	40/ 13.5	34.7	114	1814.4	4000	18.3/ 18.3	60/ 60	PC ign-meta rock	R	-	-	-	-
83	9370	20.1	66	20.1	66	0.0	0	22.7	50	20.1	66	dry Q alluv	D	8.9	11.1	-	12.2
84	9360	39.6/ 25.3	130/ 83	4.6/ 8.5	15/ 28	25.9	85	1701.0	3750	15.8/ 16.8	52/ 55	Mz meta (marble)	R	-	-	-	-
85	9280	23.2	76	18.0	59	5.2	17	136.1	300	21.6	71	wet Q alluv	A	-	53.7	-	-

Table 2B--Additional Shotpoint Information

Geo-graphic shot-point sequence no.	Shotpoint name	Hole depth (m)	Hole depth (ft)	Depth to to water before loading (m)	Depth to to water before loading (ft)	Water column in hole before loading (m)	Water column in hole before loading (ft)	Charge Size (kg)	Charge size (lbs)	Depth to top of explosive (m)	Depth to top of explosive (ft)	Surface geology	Geol. site label	South: max. dist. clear P arrival	North: max. dist. clear P arrival	South: max dist. clear energy	North: max dist clear energy
86	9244	25.9	85	25.9	85	0.0	0	294.8	650	21.3	70	wet Q alluv	A	-	-	-	-
87	9241	19.8	65	15.2	50	4.6	15	181.4	400	18.0	59	wet Q alluv	A	-	54.1	-	83.1
88	9260	21.9	72	7.0	23	14.9	49	136.1	300	19.8	65	wet Q alluv	A	-	-	-	-
89	9211	19.2	63	7.3	24	11.9	39	226.8	500	15.2	50	wet Q alluv	A	-	39.5	-	43.9
90	9212	24.7	81	24.4	80	0.3	1	453.6	1000	20.1	66	wet Q alluv	A	-	-	-	-
91	9213	23.8	78	11.6	38	12.2	40	36.3	80	22.6	74	T volc/sed	S				
92	9221	24.7	81	24.7	81	0.0	0	136.1	300	21.9	72	Mz sed	R	-	46.7	-	-
93	9222	24.7	81	24.4	80	0.3	1	136.1	300	21.3	70	Mz sed	R	-	40.9	-	75.4

Explanation:

1) "Geographic sequence number" is sequential from south to north on the main part of Line 2, followed by south to north on the 6000 and 7000 lines, followed by east to west on the 3000 and 4000 lines.

2)"Water column in hole before loading" is the difference between the two pairs of columns to the left, averaged where two holes were drilled at a single shotpoint.

3) "Surface geology" was taken from geologic maps (Jennings and Strand, 1969; Jennings 1977; Dibblee, 1967, 1992, 1996). Abbreviations are Q-Quaternary, QT- Quaternary and Pliocene, T-Tertiary, Mz-Mesozoic, PC-Precambrian, alluv-alluvium, sed-sedimentary rocks, ign-igneous rocks, meta-metamorphic rocks, volc-volcanic rocks.

4) "Geologic site labels" are A-wet alluvium (Q or QT), D-dry alluvium (Q or QT), S-sedimentary rocks (T), R-hard rock (Mz-PC).

5) "South/north maximum distances for clear P arrivals" are maximum south/north offsets from a shotpoint (in km) to which P-arrivals can be clearly picked. "South/north maximum distances for clear energy" are maximum south/north offsets from a shotpoint (in km) to which any energy can be discerned. Dashes ("-") in any of these 4 columns mean that P arrivals or energy was observed to the north or south ends of the main line (and presumably beyond). Blanks in any of these columns mean that there were problems with the shot, and no measurements were made.

6) Metric units were converted from English units. Both are given, as drilling and loading are done in English units.

Table 3. Permitting Organizations

Participating Organizations and Property Owners	Number of Shotpoints†	Number of Recorder Sites	Permits required for shotpoints	Permits required for stations
Federal Government Agencies (3)			3	3
U.S. Forest Service	21	226		
U.S. Veterans Administration	1	8		
U.S. Department of the Army*	[4]	[30]		
Total	**26**	**234**		
State Government Agencies (1)			1	1
California Department of Parks and Recreation	10	134		
Total	**10**	**134**		
Local Government Agencies (12)			12	12
L.A. City Department of Recreation and Parks	11	68		
L.A. County Department of Parks and Recreation	1	5		
L.A. County Sanitation Districts	1			
L.A. Unified School District	3	7		
L.A. Department of Water and Power		26		
L.A. County Department of Public Works	1	45		
William S. Hart School District/City of Santa Clarita	1	2		
Saugus Elementary School District	1	8		
Castaic Lake Water Agency	2	15		
Newhall Water District		5		
Whiteman Airport		4		
Los Angeles International Airport		5		
Total	**21**	**190**		
Conservation/Education Organizations (3)			3	3
Santa Monica Mountains Conservancy/ Mountains Recreation and Conservation Authority	1	17		
California State University, Northridge	3	24		
Masters College	1	2		
Total	**5**	**43**		
Commercial/Industrial Organizations (20)	**13**	**154**	13	20
Private Citizens (337)	**18**	**692**	18	337
Cumulative Total	**93**	**1447**	50	376

*Since all Army Corps lands utilized were leased to the L.A. City Department of Recreation and Parks, these figures overlap with those listed for City Parks sites.
†Sites with multiple boreholes were counted as a single shotpoint.

Table 4a. Sample trace problems

Stake no.	Inst type	Delays for SP's 8050	2 8085	3 8093	4 8310	5 9350	6 8570	7 8650	8 8720	9 9136	10 9360	11 8440	12 8060	13 8095
		DAY 1 -- Shot window 1											DAY 1 - Shot window 2	
1010	13		-70 same pattern as shot 13	-70 ±40									same pattern as shot 13	-67
1012	7	ded	-70 ok;lo-f noise; same pattern as shot 13	-82 ±30									same pattern as shot 13	-94
1013	13	noisy	-68 same pattern as shot 13										same pattern as shot 13	-91
1017	16		-55 could be structure											-67 could be strucutre
1019	13													
1020	1													rev polarity
1021	7		-34											-42
1027	16		Two IDENTIC AL traces-- DELETE ONE											Two IDENTIC AL traces-- DELETE ONE
1031	16	no sig/lo-f noise	no sig/lo-f noise	no sig/lo-f noise									no sig/lo-f noise	no sig/lo-f noise
1032	7												sig but gain problem	sig but gain problem
1038	16		-48											-40
1042	7	-50	-40	-42									-52	-36
1043	16	no sig/dc shft	no sig/dc shft	no sig/dc shft		no sig/dc shft	no sig/dc shft					dc shft	no sig/dc shft	no sig/dc shft
1046	16		-66	-67									0 IGNORE-- CLOSE TO SP	-72
1047	13													
1048	7	hi-f noise	ok											
1052	7		-60	-52								-73 uncertain	-60	-52

Table 4b. Sample trace corrections

	Shot Shotpoint	1 8050	2 8085	3 8093	4 8310	5 9350	6 8570	7 8650	8 8720	9 9136	10 9360	11 8440	12 8060	13 8095
Stake	Instr_ty	DAY 1 -- Shot window 1											DAY 1 - Shot window 2	
1005	13	-65 5	-65 5	-65 5	-65 5	-65 5	-65 5	-65 5	-65 5	-65 5	-65 5	-65 5	-73 5	-73 5
1007	7	-58 5	-58 5	-58 5	-58 5	-58 5	-58 5	-58 5	-58 5	-58 5	-58 5	-58 5	-64 5	-64 5
1009	1													
1010	13	-70 5	-70 5	-70 5	-70 5	-70 5	-70 5	-70 5	-70 5	-70 5	-70 5	-70 5	-67 5	-67 5
1012	7	3	-76 5	-76 5	-76 5	-76 5	-76 5	-76 5	-76 5	-76 5	-76 5	-76 5	-94 5	-94 5
1013	13	-68 5	-68 5	-68 5	-68 5	-68 5	-68 5	-68 5	-68 5	-68 5	-68 5	-68 5	-91 5	-91 5
1017	16	-55 5	-55 5	-55 5	-55 5	-55 5	-55 5	-55 5	-55 5	-55 5	-55 5	-55 5	-67 5	-67 5
1019	13													
1020	1	13	13	13	13	13	13	13	13	13	13	13	13	13
1021	7	-34 4	-34 4	-34 4	-34 4	-34 4	-34 4	-34 4	-34 4	-34 4	-34 4	-34 4	-42 4	-42 4
1022	16													
1031	16	2	2	2	13	13	13	13	13	13	13	13	2	2
1032	7												1	1
1038	16	-48 4	-48 4	-48 4	-48 4	-48 4	-48 4	-48 4	-48 4	-48 4	-48 4	-48 4	-40 4	-40 4
1042	7	-44 4	-44 4	-44 4	-44 4	-44 4	-44 4	-44 4	-44 4	-44 4	-44 4	-44 4	-44 4	-44 4
1043	16	2	2	2	1	2	2	1	1	1	1	3	2	2
1046	16	-66 5	-66 5	-66 5	-66 5	-66 5	-66 5	-66 5	-66 5	-66 5	-66 5	-66 5	-64 5	-64 5
1047	13													
1048	7													
1052	7	-57 5	-57 5	-57 5	-57 5	-57 5	-57 5	-57 5	-57 5	-57 5	-57 5	-57 5	-57 5	-57 5
1054	16													

Explanation:

The number at the top of each cell is the averaged time correction for a given shot window. The number below (an integer, 1-13) is a flag indicating the certainty of the time correction or the existence of a non-timing problem (see Murphy and others, in preparation).

Table 5. List of Acknowledgments

Participating Organizations, Property Owners, and LARSE Contractors	Persons
Federal Government Agencies	
U.S. Forest Service	Mike Wickman
U.S. Veterans Administration	Teresa Castillo
U.S. Department of the Army*	Karvel Bass
	Robert Colangelo
State Government Agencies	
California Department of Parks and Recreation	Rich Rozzelle
	Randy Cedarquist
California Department Industrial Relations, Division of Occupational Safety and Health	Jerel Snapp
	Stan Rhyu
Local Government Agencies	
L.A. City Bureau of Engineering	Mike Michalski
	Robert Hancock
	Linda Moore
L.A. City Department of Recreation and Parks	Jay Sloan
L.A. City Fire Department	Andrew Gutierrez
L.A. Police Department	Randy Becker
L.A. City Department of Water and Power	Richard Nagel
	Mark Mackowski
	Cliff Plumb
	Simon Hsu
L.A. City Officials	Councilperson Cindy Miscikowski
	Bob Canfield
	Ellis Stanley
	Judith Steele
	Lisa Merlino
Santa Monica City Department of Public Works	Joan Akins
L.A. County Department of Parks and Recreation	Jim Park
	Lillie Lowery
L.A. County Sanitation District	David Nakagaki
L.A. County Department of Public Works	Eric Gonzales
L.A. Unified School District	Evan Morris
William S. Hart School District/City of Santa Clarita	Mike Otavka
	Evan Aldrich
Saugus Elementary School District	Mark Fulmer
Castaic Lake Water Agency	Robert Sagehorn
	Michael Thompson

Table 5. List of Acknowledgments

Conservation/Education Organizations	
Santa Monica Mountains Conservancy/ Mountains Recreation and Conservation Authority	Jeff Bolton
California State University, Northridge	Tom Tindall
	John Chandler
	Kit Espinosa
	Judith Nutter
Masters College	Bob Hotton
	Rick Hulett
Utility	
Southern California Gas Company	Jim Montgomery
	Tom Shroeder
	Jim Mansdorfer
	Peter Sego
	Sharon O'Rouke
	Steve Cardiff
Companies	
Browning-Ferris Industries	James Aidukas
	James Ambroso
Playa Vista Development Company	Bruce Harrigan
El Cabellero Country Club	Ralph Herman
	Tom Burnsen
	Doug Meadows
Riviera Country	Gerd Koenig
	Paul Ramina
Magazine Canyon	Bruce Harrigan
Berry Petroleum Co.	Ralph McPhetridge
National Technical Systems	John Czajkowski
Capp's TV	Capp Loughboro
Richmond American Homes	Steven Seemann
The Oaks Camp and Conference Center	Dana Stewart
	Dan Smith
Calaveras Cement Company	Ed Watamaniuk
	David Whitney
California Portland Cement Company	Leo Mercy
	Steve Palmer
National Cement Company	Byron E McMichael
Private Individuals	32
LARSE Contractors	
Sam Crum Water Well Drilling, Inc.	Sam Crum
Alpha Explosives	Gordon Coleman

Appendix Ia
Shot size determination from a model curve determined with distance weighting (1/x)

90.00 percent of shots
will produce v < 1.00 in/s at this distance.

	Distance (feet)			
Shot Size (lb)	Hard Rock	Wet Alluvium	Dry Alluvium	Sed Rock
5	53	34	0	0
10	106	77	12	0
15	149	112	28	0
20	187	143	42	0
25	220	171	55	13
30	250	196	67	20
35	278	220	79	26
40	304	242	89	32
45	329	262	100	38
50	352	282	110	43
60	395	318	128	54
70	434	352	146	64
80	471	383	162	73
90	505	412	177	82
100	537	439	192	91
150	677	559	257	130
200	792	658	312	164
250	892	745	361	195
300	981	822	404	222
350	1062	892	445	248
400	1137	956	482	272
450	1206	1016	517	294
500	1270	1073	549	316
600	1389	1176	610	355
700	1496	1270	665	392
800	1594	1355	716	426
900	1685	1435	764	457
1000	1770	1510	809	487
1500	2131	1827	1001	616
2000	2423	2084	1158	724
2500	2672	2304	1294	817
3000	2892	2497	1414	900

95.00 percent of shots
will produce v < 1.00 in/s at this distance.

	Distance (feet)			
Shot Size (lb)	Hard Rock	Wet Alluvium	Dry Alluvium	Sed Rock
5	99	71	9	0
10	176	134	38	0
15	237	185	62	17
20	289	229	83	28
25	335	267	102	39
30	376	302	120	49
35	414	335	137	59
40	449	364	152	68
45	482	393	167	76
50	514	419	181	84
60	571	468	207	100
70	624	513	232	115
80	672	555	255	129
90	717	594	276	142
100	760	630	296	154
150	943	788	385	210
200	1093	919	460	258
250	1222	1031	525	300
300	1337	1131	584	338
350	1441	1222	637	373
400	1536	1305	686	406
450	1625	1382	732	436
500	1707	1455	776	465
600	1858	1587	855	518
700	1994	1706	928	567
800	2119	1816	994	612
900	2234	1917	1056	654
1000	2342	2012	1114	693
1500	2797	2413	1362	864
2000	3163	2737	1565	1004
2500	3474	3013	1738	1124
3000	3747	3255	1891	1232

Appendix Ia
Shot size determination from a model curve determined with distance weighting (1/x)

99.00 percent of shots
will produce $v \leq 1.00$ in/s at this distance.

Shot Size (lb)	Distance (feet)			
	Hard Rock	Wet Alluvium	Dry Alluvium	Sed Rock
5	245	192	65	18
10	387	312	125	52
15	496	404	173	80
20	587	482	215	104
25	666	549	251	127
30	736	610	285	147
35	800	665	316	166
40	859	716	344	184
45	914	764	371	201
50	966	809	397	217
60	1061	891	444	248
70	1147	966	487	275
80	1226	1034	527	301
90	1300	1098	564	325
100	1368	1158	600	348
150	1661	1414	751	449
200	1899	1623	877	533
250	2102	1801	985	606
300	2282	1959	1082	671
350	2443	2101	1169	731
400	2591	2231	1249	786
450	2727	2352	1324	837
500	2854	2464	1394	885
600	3085	2669	1522	974
700	3293	2853	1637	1054
800	3483	3021	1743	1128
900	3658	3176	1841	1196
1000	3820	3320	1932	1261
1500	4505	3928	2321	1535
2000	5052	4415	2634	1758
2500	5514	4828	2901	1948
3000	5918	5189	3135	2117

90.00 percent of shots
will produce $v \leq 2.00$ in/s at this distance.

Shot Size (lb)	Distance (feet)			
	Hard Rock	Wet Alluvium	Dry Alluvium	Sed Rock
5	13	0	0	0
10	43	27	0	0
15	69	47	0	0
20	91	65	0	0
25	112	82	14	0
30	131	97	21	0
35	148	112	28	0
40	165	125	34	0
45	181	138	40	0
50	195	151	46	6
60	223	174	56	14
70	249	195	67	19
80	273	215	76	25
90	296	234	86	30
100	317	252	95	35
150	411	331	135	58
200	489	398	170	78
250	557	456	201	96
300	619	509	229	113
350	675	557	256	129
400	726	601	280	144
450	774	643	303	159
500	819	682	325	172
600	903	754	366	198
700	978	819	403	221
800	1048	879	437	243
900	1112	935	470	264
1000	1173	988	500	284
1500	1431	1213	632	370
2000	1642	1397	741	442
2500	1822	1555	836	505
3000	1982	1695	921	562

Appendix Ia
Shot size determination from a model curve determined with distance weighting (1/x)

95.00 percent of shots
will produce v < 2.00 in/s at this distance.

	Distance (feet)			
Shot Size (lb)	**Hard Rock**	**Wet Alluvium**	**Dry Alluvium**	**Sed Rock**
5	39	24	0	0
10	85	60	0	0
15	123	91	18	0
20	155	117	30	0
25	184	142	41	0
30	211	164	52	11
35	236	184	61	16
40	259	204	71	22
45	281	222	80	27
50	301	239	88	31
60	339	271	104	40
70	375	301	119	49
80	407	329	134	57
90	438	355	147	65
100	467	379	160	72
150	592	486	217	106
200	696	575	266	136
250	786	653	309	162
300	867	722	348	187
350	940	786	384	209
400	1007	844	417	230
450	1070	898	448	250
500	1128	949	478	269
600	1236	1043	532	304
700	1333	1128	582	337
800	1422	1206	627	367
900	1505	1278	670	395
1000	1583	1346	711	422
1500	1913	1635	884	538
2000	2180	1869	1027	634
2500	2408	2070	1150	718
3000	2608	2247	1259	793

99.00 percent of shots
will produce v < 2.00 in/s at this distance.

	Distance (feet)			
Shot Size (lb)	**Hard Rock**	**Wet Alluvium**	**Dry Alluvium**	**Sed Rock**
5	128	95	20	0
10	218	170	55	13
15	290	229	83	29
20	350	280	109	43
25	403	325	132	56
30	451	365	153	68
35	494	403	172	79
40	535	437	191	90
45	572	469	208	101
50	608	500	225	110
60	674	556	255	129
70	733	608	284	147
80	789	655	310	163
90	840	700	335	179
100	888	741	359	193
150	1095	921	461	259
200	1265	1068	547	314
250	1410	1195	621	363
300	1539	1308	688	407
350	1656	1410	749	447
400	1763	1503	805	484
450	1862	1590	857	519
500	1954	1671	906	552
600	2123	1819	996	613
700	2275	1953	1078	669
800	2414	2076	1153	720
900	2542	2189	1223	768
1000	2662	2295	1289	813
1500	3168	2742	1568	1006
2000	3575	3102	1794	1164
2500	3920	3408	1988	1300
3000	4222	3677	2160	1421

Appendix Ia
Shot size determination from a model curve determined with distance weighting (1/x)

90.00 percent of shots
will produce v < 5.00 in/s at this distance.

	Distance (feet)			
Shot Size (lb)	Hard Rock	Wet Alluvium	Dry Alluvium	Sed Rock
5	0	0	0	0
10	0	0	0	0
15	12	0	0	0
20	23	10	0	0
25	33	18	0	0
30	42	26	0	0
35	51	33	0	0
40	59	39	0	0
45	67	46	0	0
50	74	52	0	0
60	89	63	0	0
70	103	74	11	0
80	115	85	16	0
90	128	95	20	0
100	139	104	24	0
150	191	147	44	0
200	236	184	61	16
250	275	217	77	25
300	311	247	92	33
350	344	275	106	41
400	374	301	119	49
450	403	325	132	56
500	430	348	144	63
600	480	391	166	76
700	526	430	187	88
800	569	466	206	99
900	608	500	225	111
1000	646	532	242	121
1500	806	671	319	168
2000	939	785	383	209
2500	1054	884	440	245
3000	1155	973	491	278

95.00 percent of shots
will produce v < 5.00 in/s at this distance.

	Distance (feet)			
Shot Size (lb)	Hard Rock	Wet Alluvium	Dry Alluvium	Sed Rock
5	0	0	0	0
10	20	7	0	0
15	38	23	0	0
20	54	35	0	0
25	69	47	0	0
30	83	58	0	0
35	96	69	8	0
40	108	79	13	0
45	119	88	17	0
50	131	97	21	0
60	152	114	29	0
70	171	130	36	0
80	189	146	43	0
90	207	160	50	10
100	223	174	56	14
150	295	234	86	30
200	356	286	111	44
250	410	331	135	57
300	458	372	156	70
350	503	410	176	82
400	544	445	195	93
450	582	478	212	103
500	618	508	229	113
600	684	565	260	132
700	745	618	289	150
800	801	666	316	167
900	853	711	341	182
1000	902	753	365	197
1500	1111	934	469	264
2000	1283	1084	556	320
2500	1430	1212	631	369
3000	1561	1326	699	414

Appendix Ia
Shot size determination from a model curve determined with distance weighting (1/x)

99.00 percent of shots
will produce v < 5.00 in/s at this distance.

	Distance (feet)			
Shot Size (lb)	Hard Rock	Wet Alluvium	Dry Alluvium	Sed Rock
5	40	24	0	0
10	86	61	0	0
15	124	92	19	0
20	157	119	31	0
25	187	144	42	0
30	214	166	53	11
35	239	187	63	17
40	262	206	72	22
45	284	225	81	27
50	305	242	90	32
60	343	274	106	41
70	379	304	121	50
80	412	332	135	58
90	442	359	149	66
100	472	383	162	73
150	598	491	220	108
200	702	581	269	138
250	793	659	312	164
300	874	729	352	189
350	948	793	388	212
400	1016	852	421	233
450	1079	906	453	253
500	1138	957	482	272
600	1246	1052	537	308
700	1344	1137	587	340
800	1434	1216	633	371
900	1518	1289	677	399
1000	1596	1357	717	426
1500	1927	1648	892	543
2000	2196	1884	1036	640
2500	2426	2086	1160	724
3000	2628	2264	1270	800

Appendix Ib
Shot size determination from a model curve determined with no distance weighting

90.00 percent of shots
will produce v < 1.00 in/s at this distance.

	Distance (feet)			
Shot Size (lb)	Hard Rock	Wet Alluvium	Dry Alluvium	Sed Rock
5	77	67	36	24
10	108	94	51	33
15	131	114	61	40
20	151	131	71	46
25	168	146	78	51
30	183	160	86	55
35	198	172	92	60
40	211	183	98	63
45	223	194	104	67
50	235	204	110	71
60	257	223	120	77
70	277	241	129	83
80	295	257	138	89
90	313	272	146	94
100	329	286	153	99
150	402	349	186	120
200	462	402	214	138
250	516	448	239	153
300	564	490	261	168
350	608	528	281	181
400	649	564	300	193
450	688	597	318	204
500	724	629	335	215
600	792	688	366	235
700	855	742	395	253
800	913	792	421	270
900	968	840	446	286
1000	1019	884	470	301
1500	1245	1080	573	367
2000	1436	1245	660	422
2500	1603	1390	737	471
3000	1755	1522	806	515

95.00 percent of shots
will produce v < 1.00 in/s at this distance.

	Distance (feet)			
Shot Size (lb)	Hard Rock	Wet Alluvium	Dry Alluvium	Sed Rock
5	103	90	48	31
10	144	125	67	44
15	175	152	82	53
20	201	175	94	61
25	225	195	105	68
30	245	213	114	74
35	264	230	123	79
40	282	245	131	85
45	299	260	139	90
50	315	273	146	94
60	344	299	160	103
70	371	322	172	111
80	396	344	184	118
90	419	364	195	125
100	441	383	205	132
150	538	467	249	160
200	620	538	287	184
250	692	600	320	205
300	756	657	350	224
350	816	708	377	242
400	871	756	402	258
450	924	802	426	273
500	973	844	449	287
600	1064	924	491	314
700	1149	997	529	339
800	1227	1064	565	361
900	1300	1128	598	383
1000	1370	1188	630	403
1500	1675	1452	769	491
2000	1932	1675	886	566
2500	2158	1871	989	631
3000	2363	2048	1082	691

Appendix Ib
Shot size determination from a model curve determined with no distance weighting

99.00 percent of shots
will produce v < 1.00 in/s at this distance.

	Distance (feet)			
Shot Size (lb)	Hard Rock	Wet Alluvium	Dry Alluvium	Sed Rock
5	177	154	82	53
10	247	215	115	74
15	301	262	140	90
20	346	301	161	104
25	386	336	179	115
30	422	367	196	126
35	455	396	211	136
40	486	422	225	145
45	515	447	239	153
50	542	471	251	161
60	593	515	275	176
70	640	555	296	190
80	683	593	316	203
90	724	628	335	215
100	762	662	352	226
150	931	808	429	275
200	1072	931	494	316
250	1197	1039	551	353
300	1310	1137	603	386
350	1414	1227	650	416
400	1511	1310	694	444
450	1602	1389	736	470
500	1687	1463	775	495
600	1847	1602	848	541
700	1994	1729	915	584
800	2131	1847	977	623
900	2259	1958	1035	661
1000	2381	2064	1090	696
1500	2914	2525	1332	849
2000	3364	2914	1536	979
2500	3760	3257	1716	1093
3000	4119	3568	1878	1195

90.00 percent of shots
will produce v < 2.00 in/s at this distance.

	Distance (feet)			
Shot Size (lb)	Hard Rock	Wet Alluvium	Dry Alluvium	Sed Rock
5	51	44	24	16
10	71	62	33	22
15	86	75	41	26
20	99	86	47	30
25	111	96	52	34
30	121	105	57	37
35	130	113	61	39
40	139	121	65	42
45	147	128	69	44
50	155	134	72	47
60	169	147	79	51
70	182	158	85	55
80	194	169	91	58
90	206	179	96	62
100	216	188	101	65
150	263	229	123	79
200	303	263	141	91
250	338	294	157	101
300	369	321	172	110
350	398	346	185	119
400	425	369	197	127
450	450	391	209	134
500	474	412	220	141
600	518	450	240	154
700	559	486	259	166
800	597	518	276	177
900	632	549	293	188
1000	666	578	308	198
1500	813	706	376	241
2000	937	813	432	277
2500	1046	907	482	309
3000	1144	993	527	337

Appendix Ib
Shot size determination from a model curve determined with no distance weighting

95.00 percent of shots
will produce v < 2.00 in/s at this distance.

	Distance (feet)			
Shot Size (lb)	Hard Rock	Wet Alluvium	Dry Alluvium	Sed Rock
5	68	59	32	21
10	95	83	45	29
15	115	100	54	35
20	133	115	62	40
25	148	128	69	45
30	161	140	75	49
35	174	151	81	52
40	185	161	87	56
45	196	171	92	59
50	207	180	96	62
60	226	196	105	68
70	243	212	113	73
80	260	226	121	78
90	275	239	128	82
100	289	252	135	87
150	353	307	164	105
200	406	353	188	121
250	453	393	210	135
300	495	430	229	147
350	534	464	247	159
400	570	495	264	169
450	604	524	280	179
500	636	552	294	189
600	695	604	322	206
700	750	651	347	222
800	801	695	370	237
900	849	737	392	251
1000	894	776	413	264
1500	1092	948	503	322
2000	1259	1092	579	371
2500	1406	1219	647	413
3000	1539	1334	707	452

99.00 percent of shots
will produce v < 2.00 in/s at this distance.

	Distance (feet)			
Shot Size (lb)	Hard Rock	Wet Alluvium	Dry Alluvium	Sed Rock
5	116	101	54	35
10	162	141	76	49
15	198	172	92	60
20	227	198	106	68
25	253	220	118	76
30	277	241	129	83
35	299	260	139	89
40	319	277	148	95
45	338	293	157	101
50	355	309	165	106
60	388	338	180	116
70	419	364	194	125
80	447	388	207	133
90	474	411	220	141
100	499	433	231	149
150	608	528	282	181
200	701	608	324	208
250	782	679	361	232
300	855	742	395	253
350	923	801	426	273
400	986	855	455	291
450	1045	907	482	308
500	1100	955	507	325
600	1204	1045	554	355
700	1299	1127	598	383
800	1388	1204	638	408
900	1472	1276	677	433
1000	1550	1345	712	455
1500	1896	1644	870	555
2000	2187	1896	1002	640
2500	2444	2118	1119	714
3000	2676	2319	1224	781

Appendix Ib
Shot size determination from a model curve determined with no distance weighting

90.00 percent of shots
will produce v < 5.00 in/s at this distance.

	Distance (feet)			
Shot Size (lb)	Hard Rock	Wet Alluvium	Dry Alluvium	Sed Rock
5	30	26	14	9
10	41	36	19	13
15	50	44	24	15
20	57	50	27	18
25	64	56	30	19
30	70	61	33	21
35	75	65	35	23
40	80	70	38	24
45	85	74	40	26
50	89	78	42	27
60	97	85	46	30
70	105	91	49	32
80	112	97	52	34
90	118	103	55	36
100	124	108	58	38
150	151	132	71	46
200	174	151	81	52
250	194	169	91	58
300	212	184	99	64
350	228	198	106	69
400	244	212	114	73
450	258	224	120	77
500	271	236	126	81
600	297	258	138	89
700	320	278	149	96
800	341	297	159	102
900	362	314	168	108
1000	381	331	177	114
1500	464	403	215	138
2000	534	464	248	159
2500	596	518	276	177
3000	652	566	302	194

95.00 percent of shots
will produce v < 5.00 in/s at this distance.

	Distance (feet)			
Shot Size (lb)	Hard Rock	Wet Alluvium	Dry Alluvium	Sed Rock
5	39	34	19	12
10	55	48	26	17
15	67	58	31	20
20	76	67	36	23
25	85	74	40	26
30	93	81	44	28
35	100	87	47	30
40	107	93	50	32
45	113	98	53	34
50	119	103	56	36
60	130	113	61	39
70	140	122	65	42
80	149	130	70	45
90	158	137	74	48
100	166	145	78	50
150	202	176	94	61
200	233	202	108	70
250	259	225	121	78
300	283	246	132	85
350	305	266	142	92
400	326	283	152	98
450	345	300	161	103
500	364	316	169	109
600	397	345	185	119
700	428	372	199	128
800	457	397	212	136
900	485	421	225	144
1000	510	443	236	152
1500	622	541	288	185
2000	717	622	331	213
2500	800	695	370	237
3000	875	760	404	259

Appendix Ib
Shot size determination from a model curve determined with no distance weighting

99.00 percent of shots
will produce v < 5.00 in/s at this distance.

	Distance (feet)			
Shot Size (lb)	Hard Rock	Wet Alluvium	Dry Alluvium	Sed Rock
5	67	58	32	20
10	94	81	44	28
15	114	99	53	34
20	131	114	61	40
25	146	127	68	44
30	159	138	74	48
35	171	149	80	52
40	183	159	85	55
45	194	168	90	58
50	204	177	95	61
60	223	194	104	67
70	240	209	112	72
80	256	223	119	77
90	271	236	126	81
100	285	248	133	86
150	348	302	162	104
200	400	348	186	120
250	446	388	207	133
300	488	424	226	145
350	526	457	244	157
400	562	488	260	167
450	595	517	276	177
500	627	545	290	186
600	686	596	317	203
700	740	642	342	219
800	790	686	365	234
900	837	727	387	248
1000	882	765	407	261
1500	1077	935	496	318
2000	1241	1077	571	366
2500	1386	1202	638	408
3000	1517	1316	697	446

Appendix II

Participating Organizations and Institutions

Organization/Institution		*Number of persons*
United States Geological Survey - (USGS)		37
Southern California Earthquake Center (SCEC)	University of Southern California – (USC)	14
	California Institute of Technology – (Caltech)	10
	University of California at Los Angeles – (UCLA)	10
	University of California at Santa Barbara – (UCSB)	5
University of Texas at El Paso - (UTEP)		9
California State University, Northridge - (CSUN)		9
Incorporated Research Institute of Seismology/Program for Array Seismic Studies of the Continental Lithosphere - (IRIS/PASSCAL)		5
GeoForschungsZentrum, Potsdam, Germany - (GFZ)		5
Geological Survey of Canada - (GSC)		4
University of Karlsruhe		4
University of Copenhagen, Denmark		3
Glendale Community College		2
Subsurface Exploration, Inc.		2
Stanford University		1
Pasadena City College		1
University of Dublin		1
URS Grenier Woodward Clyde		1
Total		**123**

LARSE II Personnel

Name		*Affiliation*
First	*Last*	
Marcos	Alvarez	IRIS/PASSCAL
Isa	Asudeh	GSC
Shirley	Baher	UCLA
Julia	Bartlakowski	U. Karlsruhe
Mark	Benthien	SCEC
Harley	Benz	USGS Golden
Steffen	Bergler	UTEP/U. Karlsruhe
Dave	Bowman	USC
Tom	Brocher	USGS Menlo Park

Tom	Burdette	USGS Menlo Park
Rufus	Catchings	USGS Menlo Park
Youlin	Chen	USC
Rob	Clayton	Caltech
Geoff	Clitheroe	USGS Menlo Park
Elizabeth	Cochran	UCSB
Dave	Cornwell	USGS Menlo Park
Coyn	Criley	USGS Menlo Park
Edward	Criley	USGS Menlo Park
David	Croker	USGS Menlo Park
Bill	Curtis	USGS Pasadena
Jocelyn	Davies	USGS Pasadena
Autumn	Davis	URS Greiner Woodward Clyde
Paul	Davis	UCLA
Dave	Delis	CSUN
Shane	Detweiler	USGS Menlo Park
Jeff	Dingler	USGS Menlo Park
Scott	Dodd	GSC
Chris	Duenas	UCLA
Leo	Eisner	Caltech
Chuck	Estabrook	USGS Menlo Park
Matt	Evans	UCLA
Javier	Favela	Caltech
Mike	Fort	IRIS/PASSCAL
Gary	Fuis	USGS Menlo Park
John	Galetzka	USGS Pasadena
Richard	Garcia	Caltech
Florian	Gawlas	USGS Menlo Park
Carrie	Glavich	UCSB
Nicola	Godfrey	USC
Lauri	Green	Glendale CC
William	Greer	UCLA
Steve	Harder	UTEP
Franz	Hauser	U. Karlsruhe
Tom	Henyey	SCEC
Brian	Hoffman	USC
Dan	Hollis	Subsurface Exploration
James	Hollis	Subsurface Exploration
Martha	House	Caltech
Gray	Jensen	USGS Menlo Park
Mandy	Johnson	Caltech
Barbara	Jones	CSUN
T.A.	Jones	CSUN
Peer	Jorgensen	U. Copenhagen
Ron	Kaderabek	USGS Menlo Park

Galen	Kaip	UTEP
Bill	Keller	Caltech
Randy	Keller	UTEP
Cameron	Kennedy	CSUN
Brian	Kerr	Stanford
Ingo	Koglin	U. Karlsruhe
Monica	Kohler	UCLA
Alex	Krimskiy	USC/Pomona Polytech
Stephanie	Kullen	USGS Menlo Park
Michael	Landes	U. Dublin
Pete	Lean	UCSB
YunFeng	Liu	USC
Stephen	Longhurst	UCLA
Jim	Luetgert	USGS Menlo Park
Aaron	Martin	UCSB
Iain	Matcham	IRIS/PASSCAL
Bob	McClearn	USGS Menlo Park
John	McRaney	SCEC
John	Meloche	GSC
Gregory	Miller	USGS Woods Hole
Walter	Mooney	USGS Menlo Park
Mohi	Munar	Caltech
Janice	Murphy	USGS Menlo Park
Jeff	Nealon	USGS Woods Hole
Dave	Okaya	USC
Karl	Otto	GFZ Potsdam
Tracy	Pattelena	Pasadena CC
ZhiGang	Peng	USC
Taylor	Perron	USGS Menlo Park
Raven	Peters	Glendale CC
Claus	Prodehl	U. Karlsruhe
Rachel	Reiley	CSUN
David	Reneau	USGS Menlo Park
Luke	Reusser	SCEC
Scott	Reynolds	UTEP
Luis	Rivera	Caltech
Erich	Roth	USGS Woods Hole
Justin	Rubinstein	UCLA
Trond	Ryberg	GFZ Potsdam
Jonathan	Saben	SCEC
Bob	Schieman	GSC
Kimberly	Schramm	UTEP
Albrecht	Schulze	GFZ Potsdam
Michael	Seiberlich	GFZ Potsdam
Russell	Sell	USGS Menlo Park

Oguz	Selvi	UTEP
Shawn	Shapiro	CSUN
Gerry	Simila	CSUN
Ray	Sliter	USGS Pasadena
Cathy	Snelson	UTEP
Anne	Sophie	UCLA
Paul	Tackley	UCLA
Mike	Taylor	USGS Menlo Park
Mary	Templeton	IRIS/PASSCAL
Uri	ten Brink	USGS Woods Hole
Hans	Thybo	U. Copenhagen
Kristina	Thygesen	U. Copenhagen
Kathryn	Van Roosendaal	CSUN
John	Van Schaack	USGS Menlo Park
Shannon	Van Wyk	USGS Pasadena
Jan	Villalobos	CSUN
Mike	Watkins	Caltech
Michael	Weber	GFZ Potsdam
Joel	Wedberg	USC
Angie	Williams	USGS Menlo Park
Jochen	Woessner	UTEP/U. Karlsruhe
Alan	Yong	USGS Pasadena
Willie	Zamorra	IRIS/PASSCAL

Appendix III--LARSE PUBLICATIONS, OPENFILE REPORTS, RECENT ABSTRACTS (THROUGH SPRING, 2001), AND VIDEOS

LARSE PUBLICATIONS

Fuis, G.S., Okaya, D.A., Clayton, R.W., Lutter, W.J., Ryberg, T., Brocher, T.M., Henyey, T.L., Benthien, M.L., Davis, P.M., Mori, J., Catchings, R.D., ten Brink, U.S., Kohler, M.D., Klitgord, K.D., and Bohannon, R.G., 1996, Images of crust beneath southern California will aid study of earthquakes and their effects: EOS Transactions American Geophysical Union, V. 77, p. 173, 176.

Fuis, G.S., Brocher, T.M., Mori, J., Catchings, R.D., ten Brink, U.S., Klitgord, K.D., Bohannon, R.G., Okaya, D.A., Clayton, R.W., Henyey, T.L., Benthien, M.L., Davis, P.M., Kohler, M.D., Lutter, W.J., and Ryberg, T., 1997, Defining subsurface structure in earthquake country: Earth in Space, v. 9, pp. 7-10. (This magazine is published by AGU for high-school teachers and students.)

Fuis, G.S., 1998, West margin of North America--a synthesis of recent seismic transects: Tectonophysics, v. 288, p. 265-292.

Fuis, G.S., Ryberg, T., Godfrey, N.J., Okaya, D.A., and Murphy, J.M., 2001, Crustal structure and tectonics from the Los Angeles basin to the Mojave Desert, southern California, Geology, v. 29, p. 15-18.

Fuis, G.S., Ryberg, T., Lutter, W.J., and Ehlig, P.L., 2001, Seismic mapping of shallow fault zones in the San Gabriel Mountains from the Los Angeles Region Seismic Experiment, Southern California, Journal of Geophysical Research, v. 106, p. 6549-6568.

Gao, S., H. Liu, P. M. Davis, and L. Knopoff, Localized amplification of seismic waves and correlation with damage due to the Northridge earthquake: Evidence for focusing in Santa Monica, Bull. Seism. Soc. Amer., Vol. 86, No. 1B, Northridge Earthquake special issue, Editors K. Aki and T. L. Teng., pp. S209-S230, February, 1996.

Godfrey, N.J., G.S. Fuis, V. E. Langenheim, D.A. Okaya, and T.M. Brocher, Lower-crustal deformation beneath the Transverse Ranges, southern California: Results from the Los Angeles Region Seismic Experiment, Journal of Geophysical Research (in press).

Henyey, T.L., Fuis, G.S., Benthien, M.L., Burdette, T.R., Christofferson, S.A., Clayton, R.W., Criley, E.E., Davis, P.M., Hendley, J.W., II, Kohler, M.D., Lutter, W.J., McRaney, J.K., Murphy, J.M., Okaya, D.A., Ryberg, T., Simila, G., and Stauffer, P.H., 1999, The “LARSE” Project--working toward a safer future for Los Angeles, U.S. Geological Survey Fact Sheet 110-99, 2 p.

Henyey, T.L., Fuis, G.S., Anima, R.J., Barrales-Santillo, A., Benthien, M.L., Burdette, T.R., Christofferson, S.A., Clayton, R.W., Criley, E.E., Davis, P.M., Hendley, J.W., II, Kohler, M.D., Lutter, W.J., McRaney, J.K., Murphy, J.M., Okaya, D.A., Ryberg, T., Simila, G., and Stauffer, P.H., 1999, El proyecto sísmico “LARSE”--Trabajando hacia un futuro con mas seguridad para Los Angeles, U.S. Geological Survey Fact Sheet 111-99, 2 p.

Kohler, M. D. and Davis, P. M., 1997, Crustal thickness variations in Southern California from Los Angeles Region Seismic Experiment passive phase teleseismic travel times, Bull. Seis. Soc. Am., v. 87, p.1330-1344,

Kohler, M. D., J. E. Vidale, and P. M. Davis, 1997, Complex scattering within D" observed on the very dense Los Angeles Region Seismic Experiment passive array, Geophys. Res. Lett., v. 24, p. 1855-1858.

Kohler, M. D., 1999, Lithospheric deformation beneath the San Gabriel Mountains in the southern California Transverse Ranges, J. Geophys. Res., v.104, p.15025-15041.

Lutter, W.J., Fuis, G.S., Thurber, C.H., and Murphy, J.M., 1999, Tomographic images of the upper crust from the Los Angeles basin to the Mojave Desert, California: results from the Los Angeles Region Seismic Experiment, Journal of Geophysical Research, v. 104, p. 25,543-25,565.

Ryberg, T., and Fuis, G.S., 1998, The San Gabriel Mountains bright reflective zone: possible evidence of young mid-crustal thrust faulting in southern California: Tectonophysics, v. 286, pp. 31-46.

ten Brink, U.S., Zhang, J., Brocher, T.M., Okaya, D.A., Klitgord, K.D., and Fuis, G.S., 2000, Geophysical evidence for the evolution of the California Inner Continental Borderland as a metamorphic core complex: Journal of Geophysical Research, v. 105, p. 5835-5857.

Zhu, L., 2000, Crustal Structure across the San Andreas Fault, Southern California from Teleseismic Converted Waves, Earth and Planetary Science Letters, v. 179, p. 183-190.

LARSE-RELATED PUBLICATION

Houseman, G. A., E. A. Neil, and M. D. Kohler, 2000, Lithospheric instability beneath the Transverse Ranges of California, Journal Geophysical Research, v. 105, p. 16,237-16,250.

OPEN-FILE REPORTS

Brocher, T.M., Clayton, R.W., Klitgord, K.D., Bohannon, R.G., Sliter, R., McRaney, J.K., Gardner, J.V., and Keene, J.B., 1995, Multichannel seismic-reflection profiling on the R/V Maurice Ewing during the Los Angeles Region Seismic Experiment (LARSE), California: USGS Open File Report 95-228, 70 p., 3 pl.

Gao, S., Liu, H., Davis, P.M., Knopoff, L., and Fuis, G., 1996, A 98-station seismic array to record aftershocks of the 1994 Northridge, California, earthquake: U.S. Geological Survey Open-File Report 96-690, 28 p.

Kohler, M.D., Davis, P.M., Liu, H., Benthien, M., Gao, S., Fuis, G.S., Clayton, R.W., Okaya, D., and Mori, J., 1996, Data report for the 1993 Los Angeles Region Seismic Experiment (LARSE 93), southern California: a passive study from Seal Beach northeastward through the Mojave Desert: U.S. Geological Survey Open-File Report 96-85, 82 p.

Kohler, M.D., B.C. Kerr, and P.M. Davis, 2000, The 1997 Los Angeles basin passive seismic experiment--a dense, urban seismic array to investigate basin lithospheric structures, U.S. Geological Survey Open-File Report 00-148, 109 pp.

Kohler, M. D., and B. C. Kerr, (in preparation), Data report for the 1998-1999 Los Angeles Region Seismic Experiment II Passive Array, to be submitted as a U.S. Geological Survey Open-File Report.

Langenheim, V.E., and R.C. Jachens, 1996, Gravity data collected along the Los Angeles Regional Seismic Experiment (LARSE) and a preliminary mmodel of the regional density variations in basement rocks, southern California, U.S. Geological Survey Open-File Report 96-682, 25 p.

Langenheim, V.E., 1999, Gravity and Aeromagnetic models along the Los Angeles Region Seismic Experiment (Line 1), California, U.S. Geological Survey Open-File Report 99-388, 22 p.

Murphy, J.M., Fuis, G.S., Ryberg, T., Okaya, D.A., Criley, E.E., Benthien, M.L., Alvarez, M., Asudeh, I., Kohler, W.M., Glassmoyer, G.N., Robertson, M.C., and Bhowmik, J., 1996, Report for explosion data acquired in the 1994 Los Angeles Region Seismic Experiment (LARSE94), Los Angeles, California: U.S. Geological Survey Open-File Report 96-536, 120 p.

Murphy, Janice M., Gary S. Fuis, David A. Okaya, Kristina Thygesen, Shirley A. Baher, Galen Kaip, Michael D. Fort, Isa Asudeh, (in preparation), Report for borehole explosion data acquired in the 1999 Los Angeles Region Seismic Experiment (LARSE II), Southern California: Part II DATA: U.S. Geological Survey Open-File Report.

Okaya, D.A., Bhowmik, J., Fuis, G.S., Murphy, J.M., Robertson, M.C., Chakraborty, A., Benthien, M.L., Hafner, K., and Norris, J.J., 1996, Report for air-gun data acquired at onshore stations during the 1994 Los Angeles Region Seismic Experiment (LARSE), California: U.S. Geological Survey Open-File Report 96-297, 224 p.

Okaya, D.A., Bhowmik, J., Fuis, G.S., Murphy, J.M., Robertson, M.C., Chakraborty, A., Benthien, M.L., Hafner, K., and Norris, J.J.,1996, Report for local earthquake data acquired at onshore stations during the 1994 Los Angeles Region Seismic Experiment (LARSE), California: U.S. Geological Survey Open-File Report 96-509, 332 p.

ten Brink, U.S., Drury, R.M., Miller, G.K., Brocher, T. M., and Okaya, D.A., 1996, Los Angeles Region Seismic Experiment (LARSE), California off-shore seismic refraction data: USGS Open-File Report 96-27, 29 p..

RECENT ABSTRACTS

Baher, S.A., Davis, P.M., Fuis, G., 1999, LARSE II Santa Monica high resolution survey: preliminary observations(abs.), EOS Transactions American Geophysical Union, v. 80, p. F714.

Baher, S.A., and Davis, P.M., 2000, Site response in the Santa Monica Area--The LARSE II high resolution seismic survey (HRESS) (abs.), Seismological Research Letters, v. 71, p. 242.

Baher, S.A., P. Davis, G. Fuis, and R. Clayton, 2000, LARSE II: What caused the focusing related damage in Santa Monica during the Northridge earthquake (abs.), EOS Transactions American Geophysical Union, v. 81, p. F821.

Fuis, G.S., Burdette, T.R., Criley, E.E., Murphy, J.M., Perron, J.T., Yong, A., Benthien, M.L., Baher, S.A.., Clayton, R.W., Davis, P.M., Godfrey, N.J., Henyey, T.L., Kohler, M.D., McRaney, J.K., Okaya, D.A., Simila, G., Keller, G.R., Prodehl, C., Ryberg, T., Alvarez, M., Asudeh, I., Thybo, H., and ten Brink, U.S., 1999, The Los Angeles Region Seismic Experiment, Phase II (LARSE II)--A survey to identify major faults and seismic hazards beneath a large metropolitan area (abs.), EOS Transactions American Geophysical Union, v. 80, p. F714.

Fuis, G.S., Criley, E.E., Murphy, J.M., Perron, J.T., Yong, A., Benthien, M.L., Baher, S.A.., Clayton, R.W., Davis, P.M., Godfrey, N.J., Henyey, T.L., Kohler, M.D., McRaney, J.K., Okaya, D.A., Simila, G., Keller, G.R., Prodehl, C., Ryberg, T., Thybo, H., and ten Brink, U.S., 2000, The Los Angeles Region Seismic Experiment, Phase II (LARSE II)--A survey to identify major faults and seismic hazards beneath a large urban region (abs.), Seismological Research Letters, v. 71, p. 214.

Fuis, G.S., Ryberg, T., Godfrey, N.J., and Okaya, D.A., 2000, Crustal structure and tectonics along the LARSE transects, southern California, USA(abs.), University of Copenhagen, Copenhagen, Denmark, Ninth International Symposium on Deep Seismic Profiling of the Continents and Their Margins (conf. in Ulvik, Norway, June 18-23, 2000), p. 102.

Fuis, G.S., T. Ryberg, N.J. Godfrey, D.A. Okaya, W.J. Lutter, J.M. Murphy, and V.E. Langenheim, 2000, Crustal structure and tectonics of the San Andreas fault in the central Transverse Ranges. Mojave Desert area (abs.), Stanford University Publications in Geological Sciences, Stanford, Calif., v. XXI, 3rd Conference on Tectonic Problems of the San Andreas Fault System (conf. at Stanford, Calif., Sept. 6-8, 2000).

Fuis, G.S., J.M. Murphy, W.J. Lutter,T. Ryberg, D.A. Okaya, R.W. Clayton, P.M. Davis, N.J. Godfrey, S. Baher, E. Hauksson, V.E. Langenheim, K. Thygesen, C. Prodehl, G.R. Keller, 2001, Preliminary seismic images from the Los Angeles Region Seismic Experiment, Phase II (LARSE II), southern CA (abs.), Geological Society America Abstracts with Programs, v. 33, p. A-56.

Godfrey, N.J., Fuis, G.S., and Okaya, D.A., 1999, Crustal-scale effects of compressional tectonics in southern California: results from the Los Angeles Region Seismic Experiment (LARSE) (abs.), EOS Transactions American Geophysical Union, v. 80, p. F1002.

Godfrey, N.J., Okaya, D.A., and Fuis, G.S., 2000, Lower- crustal deformation beneath the Los Angeles region, southern California: Results from LARSE Lines 1 and 2(abs.), University of Copenhagen, Copenhagen, Denmark, Ninth International Symposium on Deep Seismic Profiling of the Continents and Their Margins (conf. in Ulvik, Norway, June 18-23, 2000), p. 103.

Langenheim, V.E., and Fuis, G.S., 1999, Constraints from gravity and aeromagnetic data on interpretation of the LARSE I seismic-refraction transect, southern California(abs.), EOS Transactions American Geophysical Union, v. 80, p. F1002.

Langenheim, V.E., Jachens, R.C., Hildenbrand, T.G., Fuis, G.S. and Griscom, A., 2000, Structure of the San Fernando basin area, California, based on analysis of gravity and magnetic data, Geological Society America Abstracts with Programs, v. 33, p. A-56.

Lutter, W.J., G.S. Fuis, J.M. Murphy, D.A. Okaya, R.W. Clayton, P.M. Davis, N.J. Godfrey, T. Ryberg, C. Prodehl, G. Simila, G.R. Keller, H. Thybo, V.E.

Langenheim, N.I. Christensen, and C.H. Thurber, 2000, Preliminary tomographic images from the Los Angeles Region Seismic Experiment, Phase II (LARSE II), southern California (abs.), EOS Transactions American Geophysical Union, v. 81, p. F855.

Murphy, J.M., Fuis, G.S., Ryberg, T., Godfrey, N.J., Okaya, D.A.,2000, A movie showing the kinematics of crustal motion in the Los Angeles region, California, using a foam-rubber model, EOS Transactions American Geophysical Union, v. 81, F304.

Ryberg, T., G.S. Fuis, J.M. Murphy, D.A. Okaya, R.W. Clayton, P.M. Davis, N.J. Godfrey, C. Prodehl, G. Simila, G.R. Keller, and K. Thygesen, 2000, Preliminary reflection images from the Los Angeles Region Seismic Experiment, Phase II (LARSE II), southern California (abs.), EOS Transactions American Geophysical Union, v. 81, p. F855

Schramm, K., K.C. Miller, D. Okaya, N. Godfrey, K. van Roosendal, G. Fuis, 2000, Three-dimensional velocity model of the Los Angeles region from LARSE active source experiments (abs.), EOS Transactions American Geophysical Union, v. 81, p. F856.

Simila, G., Fuis, G., Burdette, T., Criley, E., Murphy, J., Perron, J., Yong, A., Benthien, M., Baher, S., Clayton, R., Davis, P., Godfrey, N., Henyey, T., Kohler, M., McRaney, J., Okaya, D., Keller, G., Prodehl, C., Ryberg, T., Alvarez, M., Asudeh, I., Thybo, H., ten Brink, U., 2000, The Los Angeles Region Seismic Experiment, Phase II (LARSE II): A survey to identify major faults and seismic hazards beneath a large metropoliton area, American Association of Petroleum Geologists.

Simila, G., K. Thygesen, G.S. Fuis, H. Thybo, J.M. Murphy, and D.A. Okaya, 2001, Preliminary velocity model of the upper part of the San Fernando Valley sedimentary basin (abs.), Geological Society America Abstracts with Programs, v. 33, p. A-56.

Thygesen, K., G.S. Fuis, J.M. Murphy, D.A. Okaya, V.E. Langenheim, G. Simila, H. Thybo., 2000, Preliminary velocity modeling in the San Fernando Valley: Results from the Los Angeles Region Seismic Experiment, Phase II (LARSE II), southern California (abs.), EOS Transactions American Geophysical Union, v. 81, p. F855.

VIDEOS

Video Tape "The Los Angeles Region Seismic Experiment" (9 min); produced jointly by SCEC and USGS, 1995.

Video Tape: "The results of the Los Angeles Region Seismic Experiment" (40 min); produced jointly by SCEC and USGS, 1997.